PREPARED FOR SUBMISSION TO JINST

Doping liquid Argon with Xenon in ProtoDUNE Single-Phase

authors

ABSTRACT: Doping of Liquid Argon TPCs (LArTPC) with a small concentration of Xenon is a well-known technique for light-shifting and eases the detection of the liquid Argon scintillation light. In this paper, we present the results of the largest doping test ever performed in a LArTPC. We carried out this special run in ProtoDUNE-SP at CERN from February to May 2020 to compensate for the light losses due to air contamination. We studied the light response of such a large TPC (770 tons of liquid Argon; fiducial mass: 400 tons) as a function of the Xenon concentration by using the ProtoDUNE Photon Detection System (PDS) and a dedicated setup installed before the run. The run was fully satisfactory: light shifting was uniform in space and stable in time, and most of the Ar-light quenched by impurities has been fully recovered. The recovery mechanism is effective even at small Xe concentrations (< 20 ppm). We were able to disentangle the Ar and Xe light using two dedicated X-Arapuca devices. In this way, we directly observed the increase of the 178 nm component created by the Xe de-excitations. Finally, the ProtoDUNE PDS combined with the Cosmic Ray Tagger allowed for the study of the detector response as a function of the track distance. As expected, the behavior is dominated by the increase of the Rayleigh length due to the presence of Xenon.

KEYWORDS: Noble liquid detectors (scintillation, ionization, double-phase); Neutrino detectors

Contents

1 Introduction

Liquid Argon Time Projection Chambers (LArTPC) are prominent in contemporary physics for the study of neutrino oscillations and the search for rare events, including Dark Matter [1–4]. This technology has been developed for more than 40 years and reached a level of sophistication that can be scaled up to multi-kilotonnes detectors. DUNE, in particular, is designing and constructing four underground modules with a fiducial mass of 10 kt each, which will be located at SURF for beam neutrino physics, atmospheric, supernovae and solar neutrino detection, and for the search of proton decay [5, 6]. In LArTPCs, the trajectories and energy deposit of charged particles are recorded by ionization losses and the corresponding electron drift toward the anode. Nonetheless, Liquid Argon (LAr) is a high-performance scintillator. It emits light in the Vacuum UltraViolet (VUV) region with a spectrum centered at $\lambda = 128$ nm and a yield of about 40000 photons/MeV at zero electric field and 21000 photons/MeV at the nominal electric field of DUNE: 500 V/cm. The scintillation light is produced by de-excitation of the singlet ($\tau_s \simeq 6$ ns) and triplet ($\tau_l \simeq 1.3$ μs) states of the unstable excited dimer Ar_2^*; their ratio depends on the energy loss mechanism and can be used for particle identification by the analysis of the pulse shape.

Detecting VUV light in liquid Argon is challenging but the physics advantages are remarkable, especially in DUNE. The scintillation light localizes in time the interactions and provides the t_0 to the TPC. It then improves by one order of magnitude (1 cm $\rightarrow$ 1 mm) the localization of the interaction vertex, with respect to the t_0 provided by the proton kicker of the neutrino beam (LBNF for DUNE). Furthermore, light collection is the main tool to trigger events that are not produced by the beam and plays a special role in triggering and recording supernovae neutrino bursts. The light is also anti-correlated with the ionization loss of the particle and can be exploited for combined charge-light calorimetry. A high light collection efficiency can outperform the TPC energy resolution, especially for low energy events.

Trapping and collection of 128 nm light is a major experimental challenge because the vast majority of materials absorbs UV light at this wavelength. VUV focusing is difficult and costly, and it achieves limited efficiencies. In addition, the Photon Detection Efficiency (PDE) of conventional photosensors – PhotoMultiplier Tubes (PMTs) or Silicon-Photomultipliers (SiPMs) – is extremely low even if the absorbing material is removed.
In DUNE, collection of argon scintillation light is achieved by trapping photons in reflective cells, featuring wavelength shifting (WLS) for conversion to visible light and a dichroic filter for the actual trapping of the shifted light. The photons are collected by means of SiPM arrays. This concept - ARAPUCA - has been tested along with other technologies in the first run of ProtoDUNE Single Phase (SP), and resulted to be the most efficient. An upgrade of the technology, the X-ARAPUCA, will be implemented on a large scale in ProtoDUNE phase-II and has been deployed in the detector for the Xe-doping campaign presented in this work.

The DUNE Photon Detection System (PDS) can be enhanced by doping LAr with Xenon at the level of few tens of ppm. Doping became mandatory at the end of the Run I of ProtoDUNE-SP because a failure in the recirculation system polluted the argon with nitrogen at the level of 5 ppm. Nitrogen quenches the Ar_2^* dimers that produce the scintillation light, reducing the yield. In order to recover this loss during the run, we injected xenon to transfer the slow component of the scintillation light (the metastable triplet state of the dimer) to the Xe before the nitrogen quenching.

Xenon light offers additional advantages, which have been investigated in literature with smaller detectors (see for instance [7–11]). First, the Xe scintillation light is peaked at λ = 178 nm, where the PDE of modern SiPMs exceeds 25%. In addition, the Xe reduces the effective Rayleigh length, increasing the uniformity of light propagation without affecting the absorption length. Finally, the Xe emission is faster than the triplet emission of Ar and shortens the overall time response of the detector.

The results obtained exceeded our expectations: the yield was fully recovered with just 10 ppm of Xe, without any effect on the charge collection efficiency. In addition, we benefited of ProtoDUNE-SP to perform a pilot run with Xe at different concentrations. The pilot run represents a milestone in the development of LArTPC, because no large-volume detectors with a fiducial (total) LAr mass comparable with that of ProtoDUNE-SP, 400 t (770 t), have ever been loaded with xenon. We then had the possibility to test the doping techniques, light yield, time stability, space uniformity and potential interference with charge collection at an unprecedented scale.

To reap this opportunity with enhanced precision, we installed an X-ARAPUCA telescope: a set of two X-ARAPUCAs located inside ProtoDUNE and triggered by plastic scintillators positioned on top of the cryostat.

This paper describes the preparation and the results of the Xe-doping run of ProtoDUNE-SP, both with the X-ARAPUCA telescope and the standard PDS. We describe these detectors in Secs. 2 and 3, respectively. The techniques to carry out a precise doping of a massive LArTPC are detailed in Sec. 2.3. The analysis of the data recorded by the X-ARAPUCA telescope is presented in Sec. 4. In this paper, we employed the entire Photon Detection System of ProtoDUNE: the ARAPUCA and the scintillation bars, both installed inside the anode planes. The results of the analysis from these detectors using an independent cosmic ray trigger are presented in Sec. 5. Finally, we used the TPC of ProtoDUNE-SP to evaluate the performance of charge collection in the presence of xenon, as discussed in Sec. 6.

2 ProtoDUNE-SP

The ProtoDUNE single-phase liquid argon time projection chamber (ProtoDUNE-SP) [12] is a full scale prototype for the first module of DUNE far detector [6]. With a total LAr mass of 0.77 kt, it is the largest single-phase LArTPC detector built to date. It is located in an extension to the EHN1 hall in CERN's North Area, where a new, dedicated charged-particle beam line was constructed as part of the CERN Neutrino Platform program. Construction and installation of ProtoDUNE-SP was completed in July 2018. Upon finalizing the commissioning, detector collected beam data in the 0.3 - 7 GeV range from August 29, 2018 to November 11, 2018. After the beam runs, during the CERN accelerator shutdown, the detector operated until July 19, 2020, collecting data with cosmics to validate the technologies for the future DUNE far detector modules, demonstrate operational stability, and perform R&D on different aspects of LArTPC technology. The use of Xe-doping presented in this paper was part of such an R&D effort and was performed before the end of operations of ProtoDUNE-SP.

2.1 Detector description

ProtoDUNE-SP TPC has 411 tons of active LAr volume with dimensions of 6.0 m × 6.9 m × 7.2 m. As shown in Fig. 1, the active volume is split into two sub-detectors, each having 3.6 m of drift length. In the middle of the detector, a cathode plane separates the two drift volumes. The cathode is biased to -180 kV and provides high voltage resulting into a 500 V/cm electric field in the drift region. On both sides of the cathode, at a distance of 3.6 m, we installed the anode planes. Each plane is made up of four layers of wire planes for charge readout. Each drift volume is read-out by 3 anode plane assemblies (APA), which constitute the anode of the TPC. We call these two sub-detectors Beam Left (BL) and Beam Right (BR) according to their position along the direction of the incoming charged-particle beam. Note, however, that the beam enters directly in the BR TPC through a dedicated beam-pipe filled with gas nitrogen. This "beam plug" reduces the amount of low-energy particles that range out before entering the fiducial volume. Each APA has a rectangular stainless steel frame 6.1 m high, 2.3 m wide, and 76 mm thick. Wires are bonded on both sides of the frame, with ±35.7° for the induction planes and vertically for the collection and grid plane. APAs are read-out by cold-electronics [13] that are mounted on the top section of the frames. Each drift region between the cathode and anode is defined by field cage modules, which feature the HV-degrader chain and ensure the uniformity of the drift field.

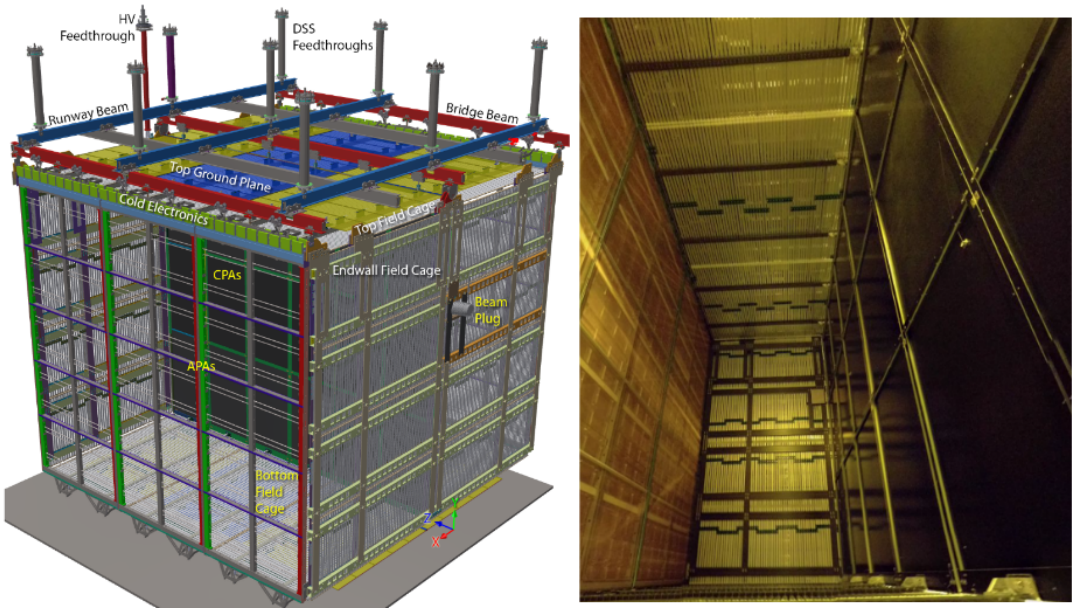

Figure 1: Left: 3D model of the ProtoDUNE-SP detector with major components labelled. Right: Photo showing one of two drift volumes where cathode is visible on the right, charge readout wire planes on the left and field cage structure surrounding the volume.

2.1.1 Photon Detection System

Photons produced by LAr scintillation are recorded by the photon detection system (PDS) modules. 10 modules, regularly spaced along the vertical direction, are inserted into each APA stainless steel frame. Each module combines a photon collector and a photon sensor. Three different module

designs, "double-shift light guides" [14], "dip-coated light guides" [15, 16], and ARAPUCA light traps [17] were realized in ProtoDUNE-SP. The location of modules in an APA frame and the three types of detector technologies are shown in Figure 2.

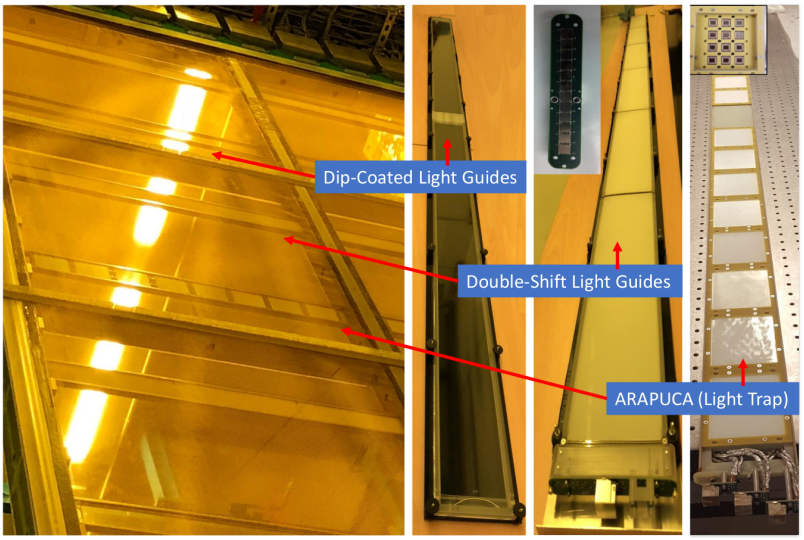

Figure 2: The three technologies of PDS modules shown inside the APA frame and on desk for comparison.

The double-shift light-guide collector combines the use of wavelength-shifting tetraphenyl-butadiene (TPB) coated radiator plates with a WLS light-guide bar. With this design, LAr scintillation light at 128 nm undergoes two wavelength-shifting steps, first to 425 nm in the plate and then to 490 nm green light in the bar. 490 nm light then is read out by photosensors placed on one end of the bar. The dip-coated collector design uses diamond-polished acrylic as the light-guide "bar". This is dipped in a solution of TPB to produce a WLS layer on the outside surface. With this concept, the initial scintillation light at 128 nm interacts with the surface coating on the bar and is shifted to 425 nm blue photons, which are later read out by a photosensor on one end of the module.

2.1.2 ARAPUCA and X-ARAPUCA

In the ARAPUCA, the trapping of VUV photons is achieved by a double shift complemented by a dichroic filter. The light is firstly wavelength shifted (WLS) from 128 to 350 nm by a p-terphenyl (pTp) coating located on top of a dichroic filter. The filter is engineered with a 400 nm cutoff so that the shifted light crosses the filter and reaches the photon trap (ARAPUCA, [17]). A second shifter absorbs the 350 nm photons, which are isotropically reemitted at 420 mn. This can be done either through a tetraphenyl-butadiene (TPB) coating or by commercial WLS light guides. The first solution is implemented in the ARAPUCA of ProtoDUNE Single Phase (SP). The second solution (X-ARAPUCA, [18, 19]) is the most efficient one; it will be implemented in the Run II of ProtoDUNE-SP and, possibly, in DUNE. The telescope used in the Xe-doping run is based on the X-ARAPUCA technology, as described in Sec. 3. In both ARAPUCA and X-ARAPUCA, the 420 nm photons are trapped inside the photon detector because the filter is reflective above the 400 nm cutoff, and they reach the photosensors (cryogenic SiPMs) bouncing in the cell or, if their

emission angle is smaller than the critical angle of the WLS bar, transported toward the SiPMs with practically no losses. The photosensors are located either in the bottom of the cell (ARAPUCA) or surround the border of the WLS plate (X-ARAPUCA).

2.1.3 Cosmic-Ray Tagger

Being on the surface, the ProtoDUNE-SP detector is exposed to 20 kHz of cosmic-ray muons, most of which are not tagged before entering the TPC. In order to tag a fraction of this particles, a Cosmic-Ray Tagger (CRT, [12]) has been installed on the upstream and downstream faces of the cryostat (and the TPC). The CRT is made of scintillator counters (strips) read by Silicon PhotoMultipliers, and it consists of four large assemblies, two mounted upstream and two downstream of the cryostat. Each assembly covers an area approximately 6.8 m high and 3.65 m wide. The combination of the information from the four assemblies allows reconstructing muon tracks crossing the TPC and produces a set of events triggered on cosmic-ray muons parallel to the APAs, whose timing and direction is well defined.

2.1.4 Cryostat

The ProtoDUNE-SP TPC is hosted in a membrane cryostat and suspended from the cryostat roof by a dedicated detector support structure. Membrane cryostat is an industrial technology used for liquefied natural gas (LNG) storage and transportation. The ProtoDUNE-SP cryostat holds 770 tons of ultra pure LAr, that is continuously purified through an ad-hoc recirculation-purification plant.

The system layout is depicted in Figure 3. It consists of two main circuits, for liquid and gas recirculation.

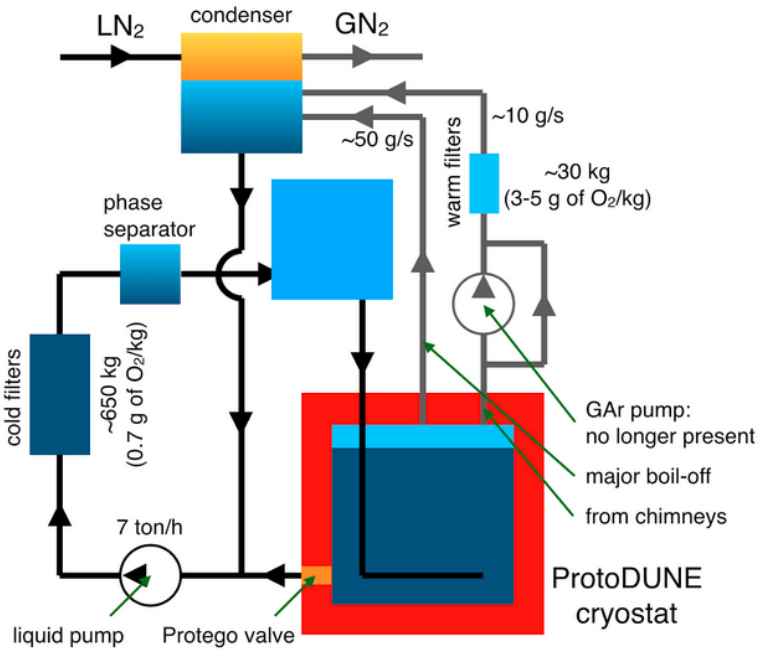

Figure 3: Schematics of ProtoDUNE-SP cryogenic system.

The first circuit extracts LAr at the bottom of one of the cryostat walls by means of a cryogenic pump. The liquid is then forced through a cold purifier at a rate of $\sim$ 7 ton/hour. The purifier consist of a first section filled with molecular sieve optimized to remove polar molecules, such as H_2O or CO_2, and a second section containing copper deposited on alumina pellets, which adsorbs O_2. The purified liquid, after passing through a phase separator, is injected back at the bottom of the cryostat at a slightly warmer temperature (and lower density) to allow its upward diffusion, thus ensuring a better mixing with the bulk LAr in the cryostat.

The second circuit works in gas phase and has two sections with two distinct functions. One is meant to stabilize the operating pressure in the cryostat by re-condensing the boil-off gas continuously produced by the residual heat input; in ProtoDUNE the mass flow rate through this section is about 42 g/s. The other part of the circuit is required to purify the gas in the ullage and in the feed-through chimneys, that is expected to be heavily polluted, more than the liquid, due to the degassing of materials (mainly the cables) present in this area. For this reason, this gas is purified a first time in the gas phase, with a smaller set of molecular-sieve/copper cartridges. Then it is condensed, together with the gas from the major boil-off. The mass flow rate through this section is about 7 g/s (a dedicated pump is installed to ensure that this flow rate is maintained, if needed).

Gas condensation is provided by a condenser continuously fed with liquid nitrogen (LN_2). The liquefied gas is sent to the input of the liquid circulation pump, where it joins the liquid extracted from the cryostat and it get purified a second time in the liquid phase.

2.2 Nitrogen contamination

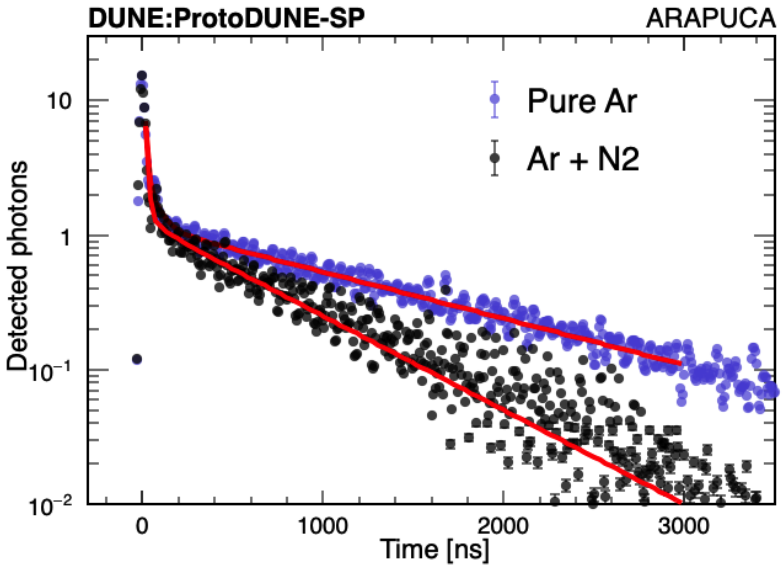

Figure 4: ProtoDUNE Arapuca module deconvoluted waveforms. Blue: "pure" Ar (before the Air contamination), Black: after air contamination and purification (only N_2 contaminant is present). Pure argon waveform is scaled to have the same maximum amplitude on both waveforms.

At the end of the Run I of ProtoDUNE-SP, a failure in the warm gas re-circulation pump leaked a certain amount of Air inside the detector. Most of the Air components, as O_2, CO_2 and H_2O, were

efficiently removed by the recirculation-purification system. However, the system cannot remove N_2, which stayed in the detector until the end of the run.

As described in Ref. [20], nitrogen affects the light output of argon through non-radiative collisional reactions ($Ar_2^* + N_2 \rightarrow 2Ar + N_2$), that destroy the argon excimers before de-excitation. This process particularly affects the long-lived triplet excimer states, effectively reducing the slow component of the Ar scintillation light.

The deconvoluted average waveforms in Figure 4 show the shape of scintillation light pulses for non-polluted LAr and LAr + N_2 after the contamination, both with electric field off. The data refer to one of the two ARAPUCA modules installed on ProtoDUNE-SP APA #6.

Measuring the reduction of the Ar Triplet scintillation light component [21] we can compute [20] the total amount of N_2 that is present in LAr: ~5.4±0.1 ppm, and derive the quantity leaked in during the accident: ~5.2±0.1 ppm. The initial (pre-accident) concentration estimated with this method is ~0.2 ppm N_2 and is compatible with the value provided by the LAr supplier (AirLiquide) and measured at the arrival of which in turn was measured to be much better that the upper limit of 2 ppm defined in the delivery contract. (Filippo is asking J. Bremer and M. Chalifour to provide the LAr delivery quality report).

2.3 Xenon doping in Liquid Argon

Doping liquid argon with xenon can enhance the response of the DUNE PDS, thanks to the more favourable physical properties of xenon scintillation light, as mentioned in Sec. 1. The effects of xenon doping were investigated on a number of small scale detectors over the years.

Xenon is a liquid cryogenic scintillator as argon and it is exploited in various direct Dark Matter search experiments [22, 23]. Indeed, its higher atomic number makes it appealing as primary target/detecting medium in dual-phase TPCs for Dark Matter searches, while such use is not feasible for much larger neutrino detectors. Xenon scintillation light is emitted at 178 nm: light detectors with high enough sensitivity at this wavelength are already commercially available (both PMTs and SiPMs), therefore xenon scintillation light can be collected quite efficiently and it allows reducing/removing other wavelength-shifting elements, like TPB. Furthermore, Xe scintillation light has two components, as argon, both much faster than the argon triplet light (4 and 22 ns), which leads to shortening the PDS time response. Finally, the Rayleigh scattering length of xenon is significantly larger than that of argon: in the framework of an experiment like DUNE, with large drift distances, this should help obtaining a more uniform yield, in terms of photons reaching the light detectors, as a function of the distance from the detectors themselves. The mentioned properties of xenon make it appealing for use as a dopant in the DUNE LAr-TPCs, and indeed a dedicated effort is going on with MonteCarlo simulations, to try and estimate the possible gain in terms of light yield and uniformity of response in the DUNE far detectors.

Xenon liquefies at 165 K and freezes at 161 K. For this reason, its dilution in argon must be performed with extreme care, in order to avoid solidification of the dopant. Usually, its concentration in previous experiments ranges from few ppm to few %, with light shifting effects setting on already at the few ppm level. According to present models, xenon atoms in suspension in liquid argon interfere with the light production process that involves the argon excited dimers Ar_2^* (see Figure 5): the non-radiative collision of a first Xe atom with the dimer leads to the formation of a new hybrid dimer $ArXe^*$, whereas the interaction of a second Xe atom yields a full transfer of energy to a Xe_2^*

dimer, which is at this point the entity decaying with emission of light, at 178 nm. The process is competitive with light quenching induced by impurities such as N_2 [24], as it affects mostly the long-lived triplet state of the argon dimer $^3\Sigma_u^+$. The time constants of the process depend directly on the Xe concentration, as well as the shape of the collected light signal.

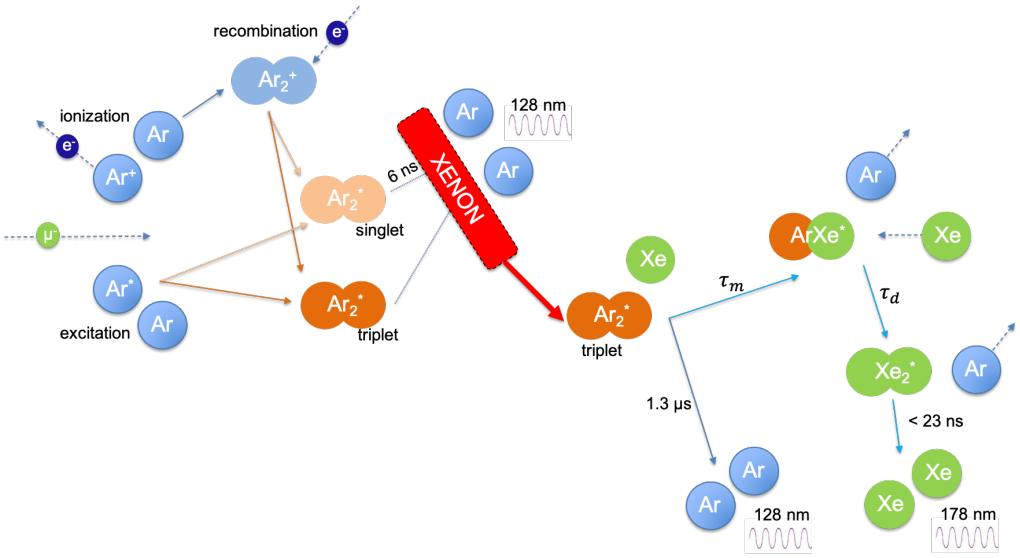

Figure 5: Sketch of the production process of scintillation light in pure liquid argon, and of the effect of xenon doping. The time constants of the non-radiative energy-transfer processes τ_m and τ_d depend on the Xe concentration in LAr.

It is presently well understood ([24] and references therein) that the presence of few ppm of Xenon in LAr already shifts a significant amount of the 128 nm LAr photons to the Xe scintillation wavelengths. In a detector like ProtoDUNE-SP, this translates into injecting few kg of xenon in the LAr bulk: for this reason, it was deemed feasible and important to use the detector as a test-bed for the study of the effects of xenon-doping at large scale. Furthermore, in this context the injection of Xenon actually helped recovering most of the light lost by the anomalous concentration of N_2, which resulted from the air leakage. Still, doping such a large detector has never been attempted before and the long-term behaviour of Xe in LAr has never been investigated at this scale.

Preliminary tests, performed by our group with smaller LAr-TPC prototypes equipped with gas recirculation/purification systems, demonstrated that Xenon can be efficiently mixed with LAr by injecting it in the gas phase. The injection can be performed at the level of the argon gas re-circulation system, at the input of the purifier and before the re-condensation. Several mixing ratios were tested showing that the Ar/Xe ratio must be above 10^3 to avoid the solidification of the Xenon on the walls of the condenser. This effect (*freeze-out*) was observed by us during the Xe-doping run on the small scale tests: at the highest Xe concentrations, the pipes of the condenser were clogged up and the Argon re-circulation stopped.

In ProtoDUNE-SP, the Xenon injection point is placed along the chimney boil-off re-circulation line (see Figure 3), after the gas purification filter but way before the condenser to allow for full mixing within the gas flow The maximum Xe mass flow rate was set to 36 g/h, to be well within the Ar/Xe ratio limit described above; this corresponds to 50 ppbm/hour in the ProtoDUNE-SP detector.

Based on the numerical (CFD) simulation of the LAr flow within the ProtoDUNE cryostat [25], the Xenon injected at this rate is expected to be uniformly distributed in LAr within few hours.

To know with good precision the amount of Xenon gas introduced in ProtoDUNE during the injection phases, the Xenon bottle was placed on a scale connected to the detector slow control system and the variation in weight were constantly recorded. After the pressure reducer on the Xe bottle, a dedicated purification filter (SAES Micro-Torr) was installed followed by a mass flow-meter, calibrated for Xenon, and a pressure gauge. A dedicated pumping system was also installed to evacuate the line between the Xenon bottle and the connection with the Argon re-circulation system. The Xenon pressure, flow and the weight of the bottle were continuously recorded by the Slow Control. Figure 6 illustrates the Xenon injection set up.

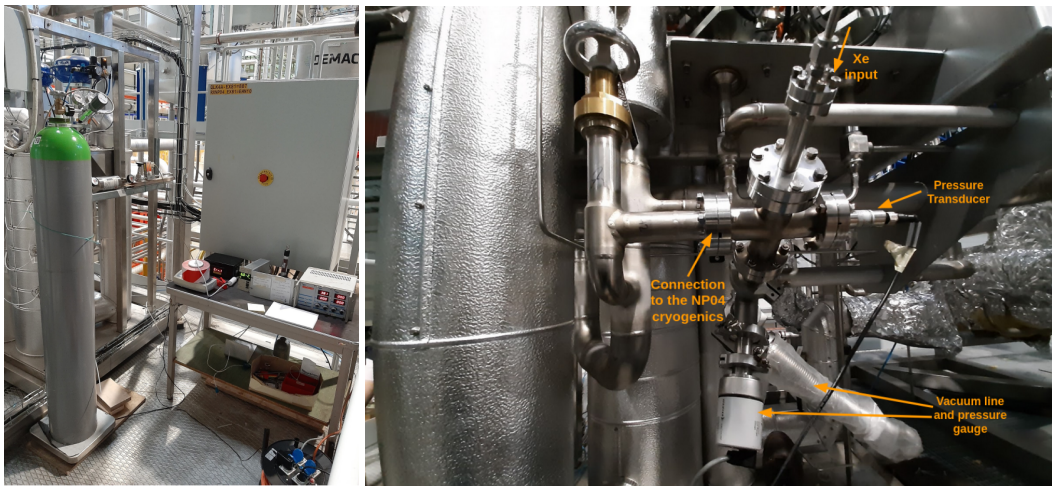

Figure 6: Left: the Xenon bottle on the scale connected to the gas purifier, the mass flow-meter and the injection line. Right: the UHV injection line equipped with vacuum/pressure monitoring devices and connected to the NP04 gas circulation system.

The Xe-doping run of ProtoDUNE-SP started in February 2020 and lasted for five months with the goals of studying light yield and efficiency in the presence of Xe, long term stability and uniformity of the doped Xe inside the cryostat. It was performed with three different bottles of Xenon.

The first bottle (containing about 3 kg of xenon) was rated with a purity grade 5.0, without any specifications on upper limits on fluorinated compounds. During the first xenon injection a sizable degradation of the free electron lifetime was recorded within the LArTPC, as shown in Figure 7.

As a consequence, the Xenon injection was stopped and a set of spectrographic/ chromatograpic analyses were performed at CERN [26]. Electro-negative impurities were identified as C_2F_6 ($\sim$ 10 ppm) plus traces of SF_6 and CO_2. These compounds, that can be present in Xenon at the ppm level as residuals of the distillation process, are known to be highly electro-negative (several order of magnitude higher that Oxygen [27]), hence they can significantly degrade the free electron-lifetime in LAr even at concentrations of few ppt.

The slow recovery of the free electron lifetime in NP04, which improved with a time constant of $\sim$30 days after the first Xenon injection, indicates that the ProtoDUNE purifiers are able to absorb

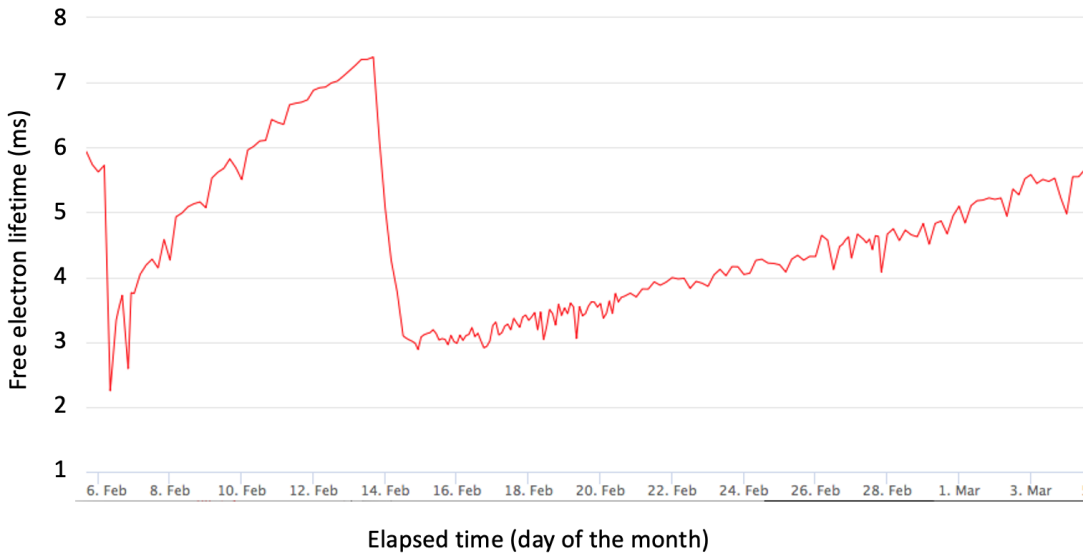

Figure 7: Left: Free electron lifetime measurement in NP04 performed with dedicated Purity monitors. The linear drop recorded around February 13th, coincides with the first Xenon injection and is attributed to the presence of fluorinated contaminants in the Xenon bottle. The subsequent recovery rate, due to LAr recirculation, is about a factor 8 to 10 slower than in previous recoveries. This suggests that the ProtoDUNE purifiers are able to absorb fluorinated compounds with an efficiency about 10 times less efficiently than that for oxygen.

fluorinated compounds with an efficiency about 10 times lower than that for oxygen.

Two additional Xenon bottles (containing about 17.5 kg each) were rated with a purity grade of 5.5 and with a specified SF_6 content, certified by the producer to be lower than 20 ppb, benefiting from the purity standard set by CERN for the ATLAS and ALICE experiments. No sizable electron lifetime degradation were observed during the subsequent injections with this higher purity Xenon.

During the run, six injections were performee (the last two are considered a single sub-run in the rest of the paper to ease the reader). The amount of Xe injected in each step and the corresponding concentration inside the cryostat is summarized in Table 1.

Table 1: Six Xe doping steps in ProtoDUNE-SP. The dates, doped Xe mass in grams and concentration in ppm by mass are given for each doping step.

Doping	Date	Doped Xe[gr]	Doped Xe[ppm]
1	13-14 February 2020	776	1.1
2	26-28 February 2020	2234	3.1
3	3-8 April 2020	5335	7.4
4	27-30 April 2020	3192	4.5
5	15-16 May 2020	400	0.6
6	18-20 May 2020	1584	2.2

Combining all the doping sub-runs, we injected 13.6 kg of Xenon into the cryostat. It corre-

sponds to 18.8 ppm of Xe concentration by mass in the 0.77 kt LAr of ProtoDUNE-SP.

Extensive data taking during each injection and between the dopings was performed, both with the ProtoDUNE photon detection system and with dedicated detectors, as thoroughly described in the following sections. The evolution of the scintillation light yield and its properties was monitored during the whole campaign, as a function of the amount of injected Xe.

3 The X-Arapuca telescope

The monitoring of the effects of the Xenon doping in LAr was performed not only with the standard ProtoDUNE-SP PDS, but also with a dedicated set of detectors introduced inside the cryostat before starting the Xe-doping run. This device is called "X-Arapuca (XA) telescope" and is shown in Fig.8.

The telescope is made of two X-ARAPUCAs (Fig.9). The former can collect both the 128 nm

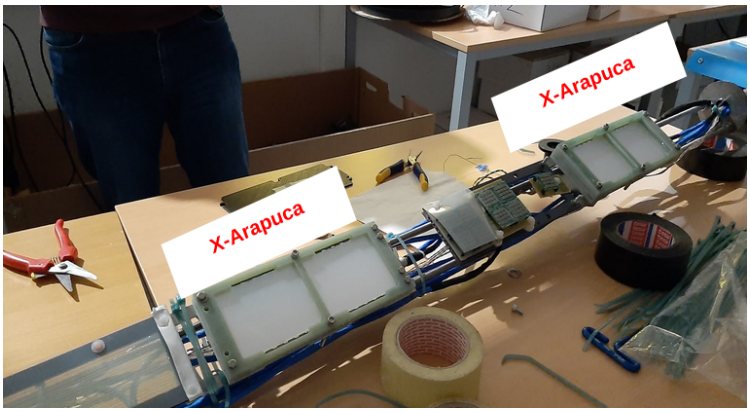

Figure 8: X-ARAPUCA detectors ready for insertion in the ProtoDUNE-SP cryostat for Xenon studies.

photons emitted by LAr and the 178 nm light shifted by Xe. The latter is a standard X-ARAPUCA covered by a fused silica window, which is opaque to the 128 nm light and records only light from Xenon. The two detectors were mounted on a mechanical support and inserted in the ProtoDUNE-SP cryostat, outside the active TPC volume, as shown in Figs.8 and 10. The telescope faces APA-6, upstream with respect to the beam, at a distance of 22.7 cm from the frame.

As mentioned above, the X-ARAPUCA is an evolution of the ARAPUCA design [18]; it is a reflective box equipped with an entrance window, two light downshifting stages, one dichroic filter and one light-guide coupled to the SiPMs. The entrance window, coated with pTP, downshifts photons from 128 nm to 350 nm with an efficiency >95%. The re-emission is isotropic; therefore, about 50% of the shifted photons enter the trap, that is flooded by LAr. The light then enters the polivinyl-toluene wavelength shifting bar installed inside the trap (EJ286® by Eljin Co.) and is absorbed and isotropically re-emitted at 440 nm. These blue photons, if emitted above the critical angle, are guided within the bar to the SiPMs, which are located at the edges of the WLS bar. Otherwise, they escape the light guide but the dichroic filter (cutoff at 400 nm) deposited on the inner side of the entrance window and the Vikuiti® reflector lining the bottom and the sides of the light trap bounce them back and forth until they are either detected by the SiPMs or absorbed by the materials of the trap.

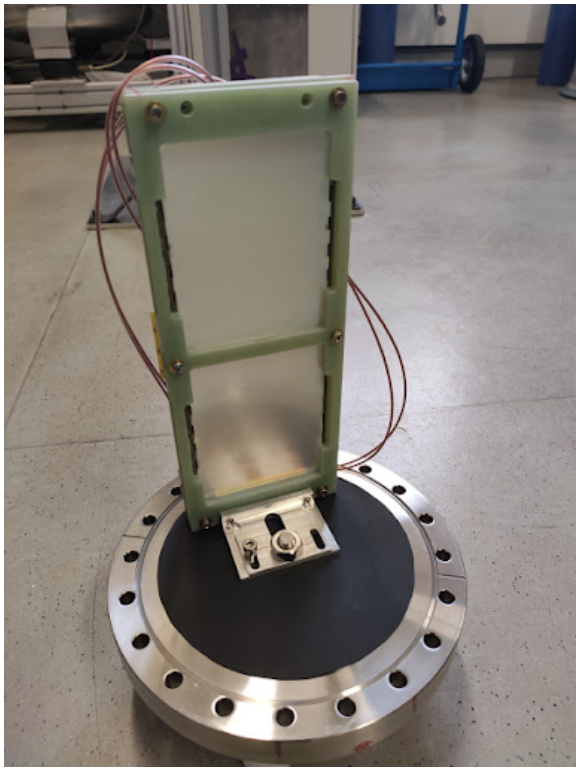

Figure 9: A closeup of one of the X-Arapuca modules, installed on a test setup.

The X-ARAPUCA device is the proposed upgrade for the first DUNE module and will be tested in 2022 during the second beam-run of ProtoDUNE-SP. Its light collection efficiency has been independently measured on two prototype devices: one sizing 10×8 cm^2 at Unicamp [28] and one double size (20×7.5 cm^2) at INFN Milano-Bicocca [19]: the latter is of the same type and size of those deployed in this work. The efficiency measurements of these two cells gives an average PDE of the X-ARAPUCA device of ~2.3%. In the Dune far detector module the X-Arapuca units are larger (48×9.3 cm^2), and are *double-sided*,i.e. the opaque bottom layer (now lined by an extended reflective foil) is replaced by entrance windows: the wavelength shifting plates will collect liquid Argon light from both half-planes.

The X-ARAPUCA devices deployed in ProtoDUNE-SP have a FR4 frame, are single-sided and feature two entrance windows produced by OPTO-Electronics Co. (Brazil)[29] (95×75 mm^2). The pTP coating was applied at Unicamp by vacuum evaporation, with a nominal thickness of ~550 μg/cm^2. The WLS bar is a single tile of $(204 \times 75 \times 4)$ mm^3, with high absorption at 350 nm and >98% emission at 440 nm [30]. The Vikuiti® film covering all internal surfaces guarantees high reflectivity (> 98%) at 440 nm. In order to cut the VUV 128 nm photons from LAr luminescence while transmitting most (85%) of the 178 nm Xenon light, one of the two X-ARAPUCAs is equipped with an additional 2 mm thick fused silica window by Opto Electronics®, located just in front of the device entrance window: this detector, which is sensitive to Xenon light only, will be labeled in the following as "Xe-XA". On the other end, the X-ARAPUCA featuring only its exposed

pTP layer fully sensitive to 128 nm photons, will be referred to as "Ar+Xe-XA".

Both XA's are equipped with Hamamatsu SiPMs S13360-6050VE [31] with a 6×6 mm^2 active area, 1.3 nF terminal capacitance and a photon detection efficiency of 35-40% at 430 nm. They were operated with a bias of 47.8 V (+4.8 V OV). This value was chosen to guarantee the SiPMs PDE efficiency >50% and to partially compensate the lack of a cold front-end amplifier that will be installed in 2022. In each module, two arrays of four SiPMs were positioned along the long sides of the WLS bar: in each array the SiPMs are readout in parallel, resulting in 4 readout channels per X-ARAPUCA. The signal of each SiPM array is delivered to the feedthrough with CAT6 cables terminated with bayonet connectors. From the flange, the same CAT6 cables deliver the signal to a custom SiPM Signal Processor (SSP) board.

The SSP [32], designed by Argonne National Laboratory for ProtoDUNE-SP Run I (2018), hosts 12 readout channels in a single board; each channel contains a fully-differential voltage amplifier and a 14-bit, 150 MSPS analog-to-digital converter (ADC) that digitizes the SiPMs waveforms. The SSP incorporates a separate power supply for each channel, providing each SiPM board with a controllable bias, up to 60 V.

The telescope is *not* triggered by the ProtoDUNE DAQ. An external trigger of cosmic rays is provided by a standard triple coincidence of 15.5×44 cm plastic scintillators, located on the cryostat roof, 1.15 m far from the active volume. This cosmic ray telescope is shown in Fig. 11. The three paddles select a solid angle of ~ 0.43 steradians, resulting in an average trigger rate of about 1 Hz. For each trigger, the DAQ collects four digitized waveforms, one per channel. The recorded waveforms are 2000 samples (13200 ns) long; they are written in an ASCII file and saved on the acquisition PC.
Fig. 12 shows the integrated statistics collected during the Xe doping campaign.

4 Analysis of the X-ARAPUCA data

Since the X-ARAPUCA data are collected with a standalone DAQ driven by the three paddles outside the cryostat, we developed dedicated algorithms for data selection analysis. At the beginning of the run, an unexpected source of noise was generated by the trigger electronics. In order to mitigate this noise, a subset of triggered events with no detectable physical signal was identified and their recorded pulses were averaged. The fraction of these empty events was approximately 7% of the total recorded triggers. We employed the averaged empty triggers to remove noise from the actual waveform and correct for the undershoot of the signal. Figure 13 shows the implementation of the noise reduction algorithm.

Prior to the physics analyses, we also performed a quality check of the stability of the light-collection system during the whole Xe-doping period. Stability is monitored by regularly extracting the response of each X-ARAPUCA channel to single photo-electrons (SPE). SPE pulses are usually searched for in the tail of each signal, i.e. well beyond the triggered pulse. The collected SPE charge distributions are fitted with a double Gaussian that models the pedestal and SPE peak. The averaged SPE waveform is extracted by selecting the subset of pulses with charge within one sigma of the mean SPE value. This average waveform represents the SPE response of the detector.

This procedure is repeated regularly over the Xe doping run. Fig. 14 displays the extracted SPE distribution for each channel, while Fig. 15 shows the SPE charge stability along the entire

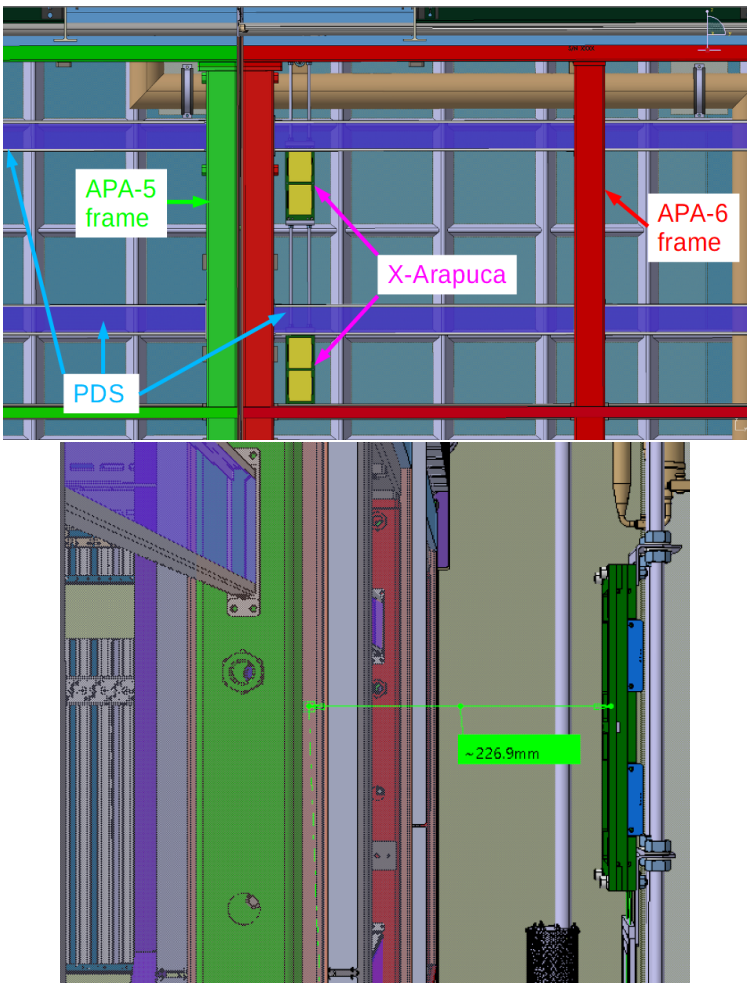

Figure 10: Top: front view of the X-Arapuca telescope inside the ProtoDUNE-SP cryostat. In green, the frame of APA-5, in red the frame of APA-6, in blue the PDS bars. Bottom: side view, showing the position of the of the X-ARAPUCAs with respect to the APA frames and PDS.

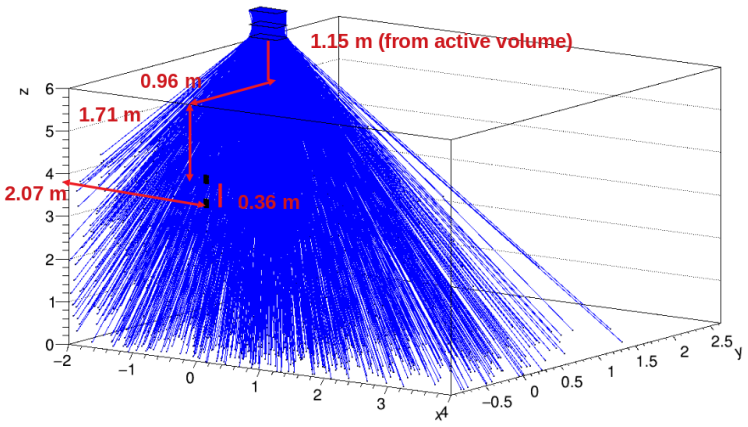

Figure 11: Position of the X-Arapuca telescope with respect to the trigger paddles.

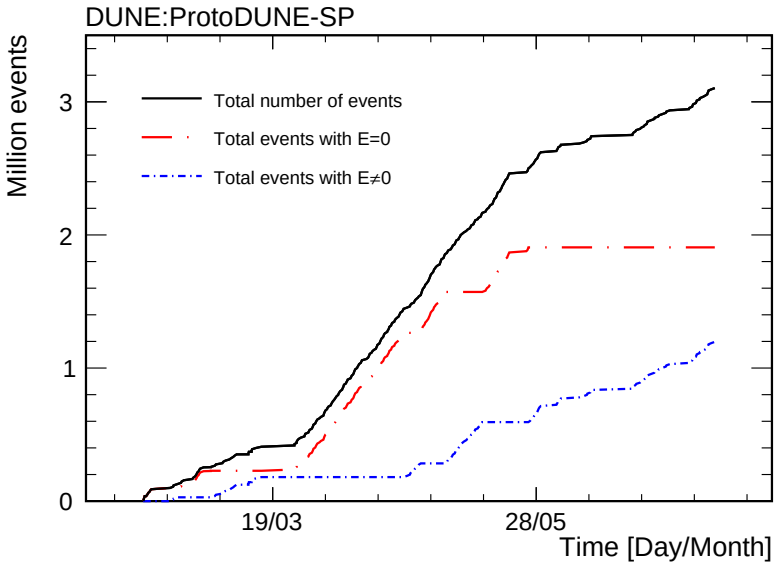

Figure 12: Total number of events acquired during the Xe doping campaign.

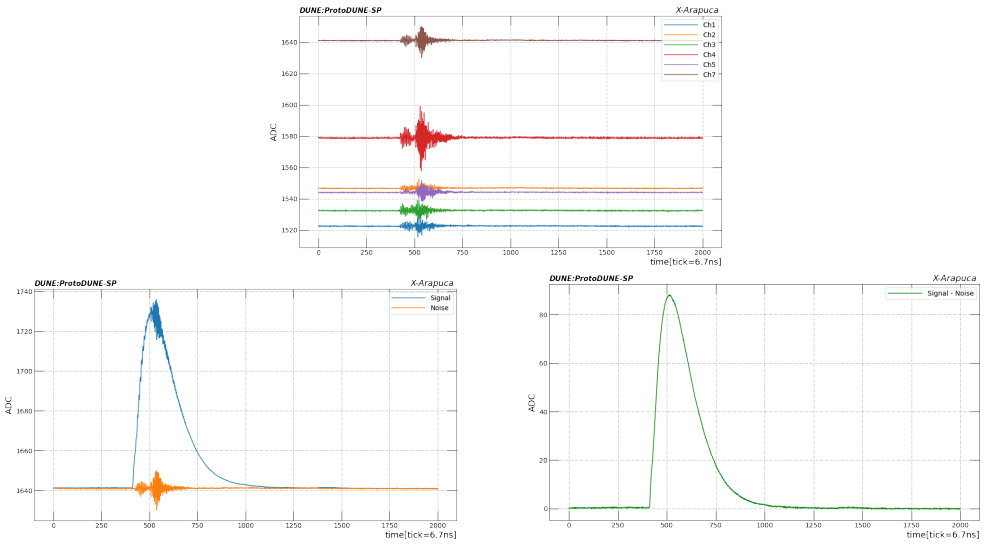

Figure 13: Mitigation algorithm for the trigger-induced noise. The top plot shows a subset of empty waveforms featuring the ripple caused by the trigger. The two bottom plots show the superposition of noise and signal waveforms, together with the noise-subtracted waveform. The units in the horizontal axis are SSP time ticks. Each tick corresponds to 6.7 ns.

run. The outcome of these quality tests demonstrated that the X-ARAPUCA system ran in stable conditions during the entire doping campaign.

4.1 Data selection and deconvolution

The data acquired with the X-ARAPUCA telescope were first converted into a ROOT TTree and pre-processed applying a moving average filter to reduce the white noise. A header recorded for

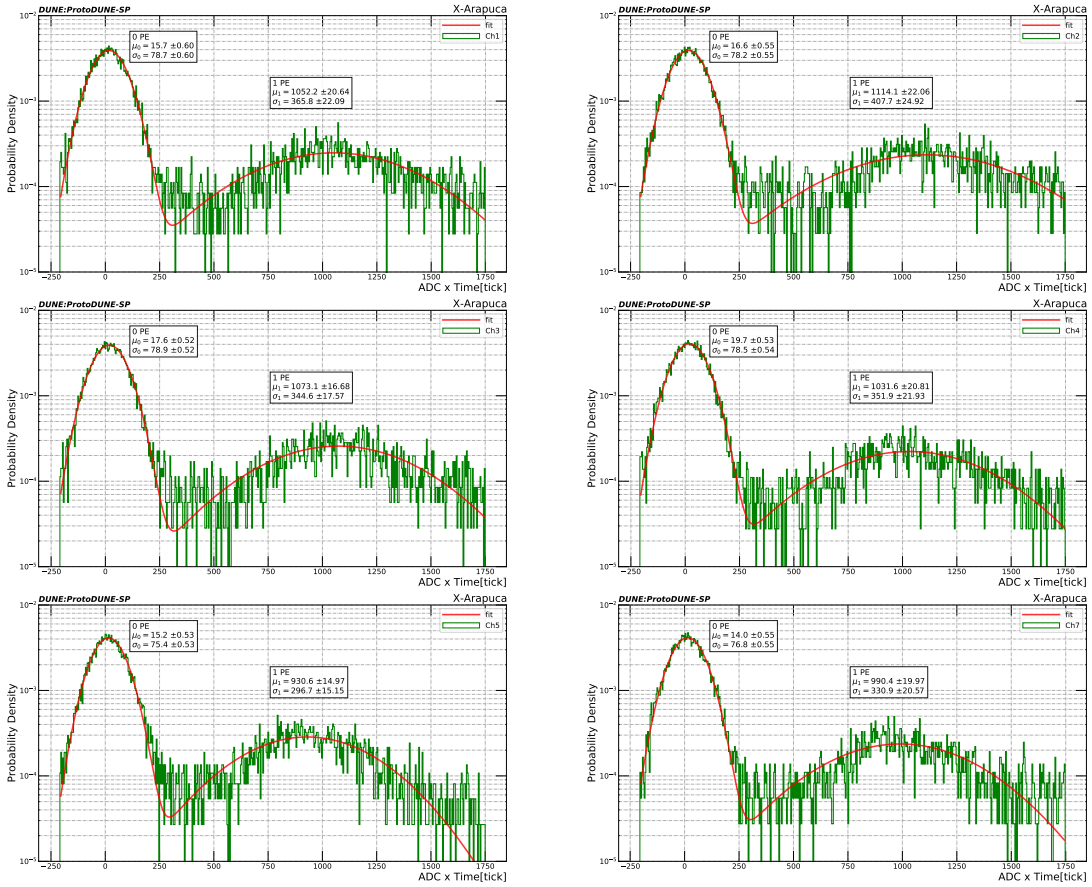

Figure 14: SPE response distribution for each XA channel fitted with a double Gaussian function to account for the pedestal and the SPE peak.

each waveform the integral, peak height in ADC counts and the absolute time when the waveform was acquired.

The data sample was selected firstly considering the peak height of the waveform, i.e. rejecting saturated events. Then, we applied a 10 photo-electron (p.e.) cut to remove events where light is present before ($1 \div 200$ ticks) or late after the trigger ($1300 \div 2000$ ticks): the event is excluded if more than 10 photo-electrons are detected in the mentioned regions of the waveform. The waveforms passing these cuts are averaged to reconstruct the transfer function, i.e. the final p.e. shape to be deconvoluted. To carry out the deconvolution, a (time-dependent) template for the single photo-electron is needed. A filter for peak finding is implemented to search single photo-electrons in the pre-trigger region. Once selected, they are aligned at the same time and averaged; the resulting shape is then fitted. The fit function consists of a double exponential convoluted with a Gaussian to account for white noise: $h(t) = Gaus(t;\mu,\sigma) \otimes (\exp[-t/\tau_1] - \exp[-t/\tau_2])$. The deconvolution technique used is based on the Gold algorithm [33] and the parameters were optimized to minimize the reconstructed fast component of LAr and the noise. Fig. 16 shows some examples of deconvoluted waveforms for each X-ARAPUCA.

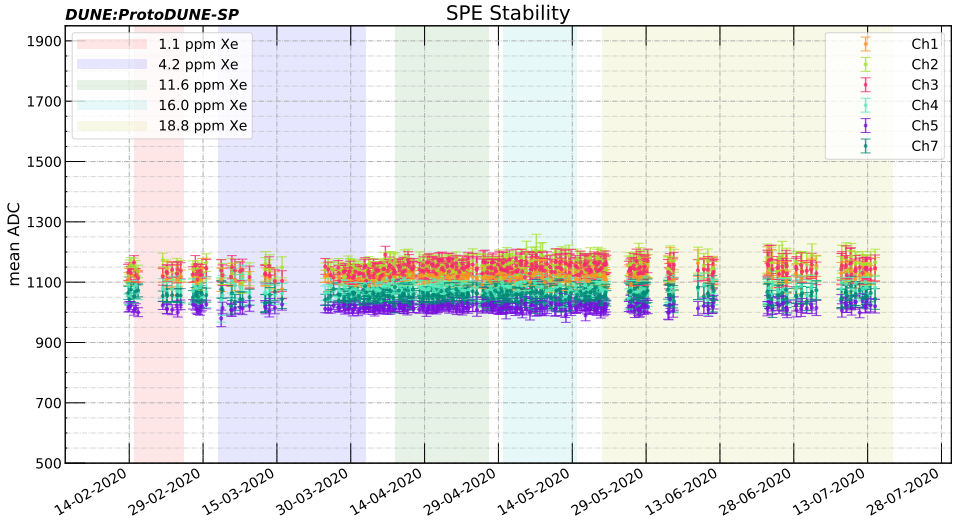

Figure 15: Mean SPE charge stability for all runs and each channel. Runs cover an overall six-month doping period, coloured areas represent specific dopings.

4.2 Effects of Xenon on LAr light

The amount of liquid Argon scintillation light (128 nm) that is shifted to Xenon light (178 nm) is the observable chosen to evaluate the efficiency of the energy transfer between Argon and Xenon excimers. The observable is the ratio between the Xenon light and the total light detected for each run, that is, the ratio of the average light seen by the Xe X-ARAPUCA (only sensitive to Xe, see Sec. 3) and the average light seen by the Ar+Xe X-ARAPUCA (sensitive to the total light).

$$\text{ratio} = \frac{\text{Xe light}}{\text{Ar light} + \text{Xe light}} \equiv \frac{\langle \gamma_{\text{Xe XA}} \rangle}{\langle \gamma_{\text{Ar+Xe XA}} \rangle} \tag{4.1}$$

This ratio is shown in Figure 17: it increases at each doping, reaching a saturation point around 0.65 for a xenon concentration greater than 16.1 ppm. The ratio remains stable outside the injection periods (dashed regions) and does not vary as a function of the electric field.

The ratio provides an estimate of the amount of Ar-light that is shifted, but does not give any information about the recovery of the light. In Fig. 18 the average number of photons detected by the X-ARAPUCA modules is presented as a function of time. It increases during each injection and remains constant during the monitoring periods. Sudden drops of the light collection values are caused by the activation of the HV system of ProtoDUNE (finite electric field), as the field prevents the full recombination of ionized Argon atoms.

Further information can be extracted by surveying the evolution over time of the fast and slow light components yield, as shown in figures 19 and 20. The slow light yield follows the expected behaviour, increasing with doping, and decreasing when the TPC electric field is on. On the other hand, in both X-ARAPUCAs, the amount of fast light swiftly drops in the first doping period.

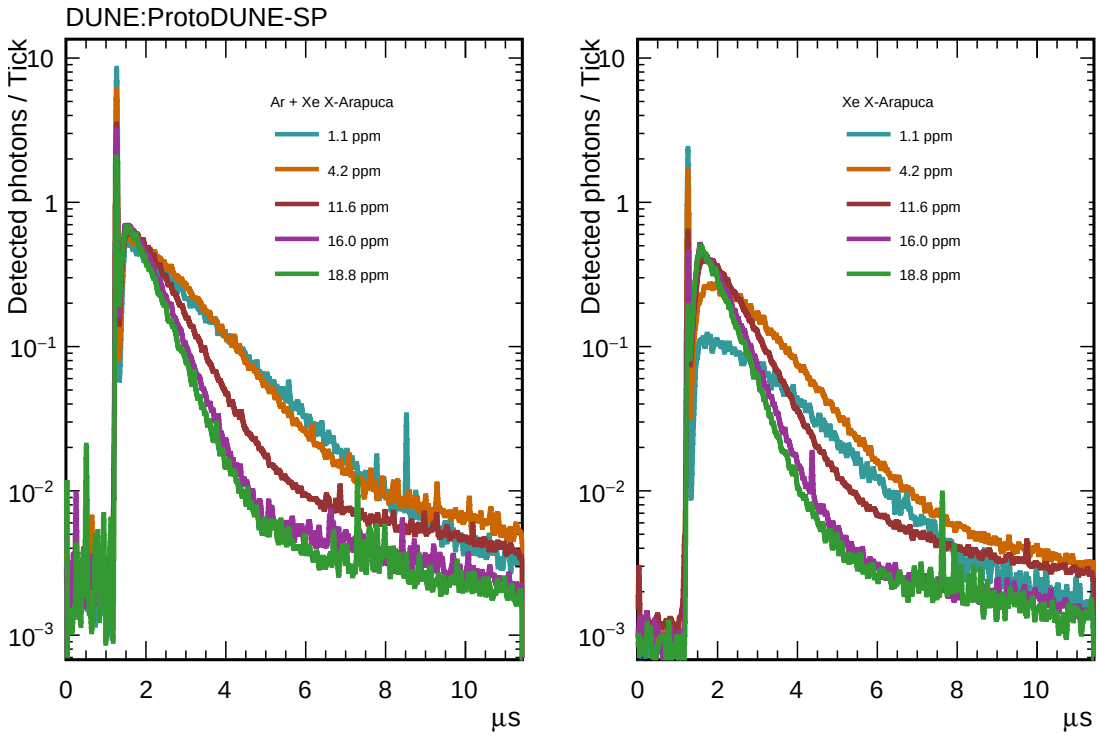

Figure 16: SPE-deconvolved average waveforms at different stages of Xe doping. Left panel: *Ar+Xe-XA*; right panel: *Xe-XA*. Only events with at least three detected photons in the Ar+Xe X-ARAPUCA module are selected.

This shows that even at 1 ppm of Xe the energy transfer from Ar_2^* to $ArXe^*$ and/or Xe_2^* dimers is ongoing even on short-lived Ar_2^* singlet states whereas – even at higher concentrations – a residual fast component remains. The residual fast light detected in the X-ARAPUCA equipped with quartz (Xe X-ARAPUCA) usually consists of one or two photons per event and it may be generated by parasitic sources like Cherenkov emission, spurious background inside the device, or shifted light escaping other PDS modules and reaching the X-ARAPUCA box.

5 Analysis of the ProtoDUNE-SP PDS

The built-in Photon Detection System (PDS) of ProtoDUNE-SP provides an independent handle by which to observe the various changes in the scintillation medium as a consequence of doping or contamination. It also has the added benefit of allowing direct comparison with the original run period, which averaged a liquid argon electron lifetime on the order of 10 ms [12]. To this end, the run periods covered in this section have multiple epochs, a period before xenon doping and nitrogen contamination described as the first ProtoDUNE-SP run period; a period after the first run, where oxygen and nitrogen were found in the scintillation volume; and a xenon doping period, where xenon was injected on the order of a few ppm, until a final concentration of 18.8 ppm [12]. The oxygen contamination was effectively removed by the replacement of a filter, but the nitrogen

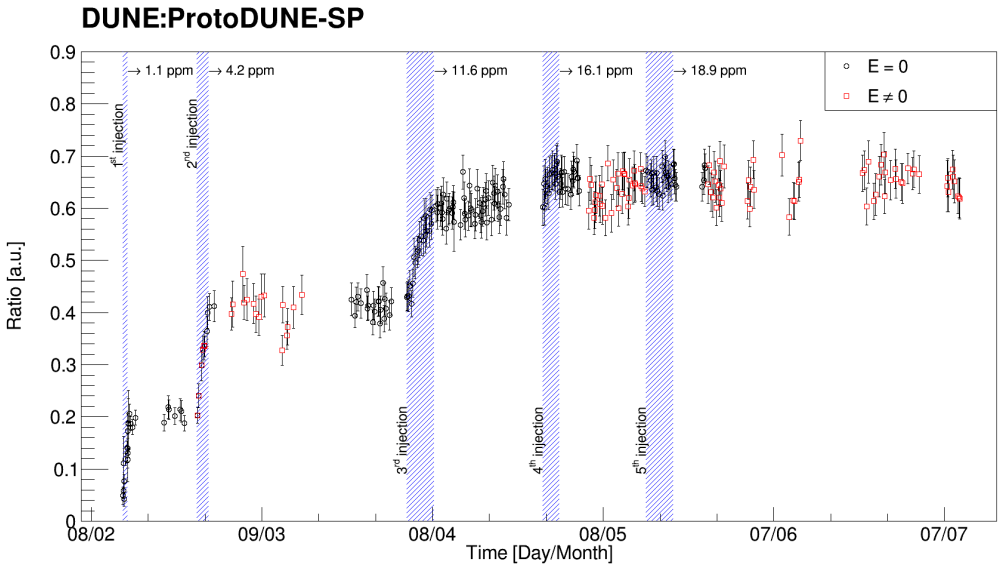

Figure 17: Fraction of the Argon light (128 nm) that is converted to Xenon Light (178 nm): $\frac{\text{Xe}}{\text{Ar+Xe}}$. The ratio increases with the doping and reaches a plateau around 0.65 for Xenon concentration greater than 16.1 ppm. The red points correspond to data collected with the nominal TPC electric field, while black points refer to data with no electric field. Shaded areas indicate Xe injections.

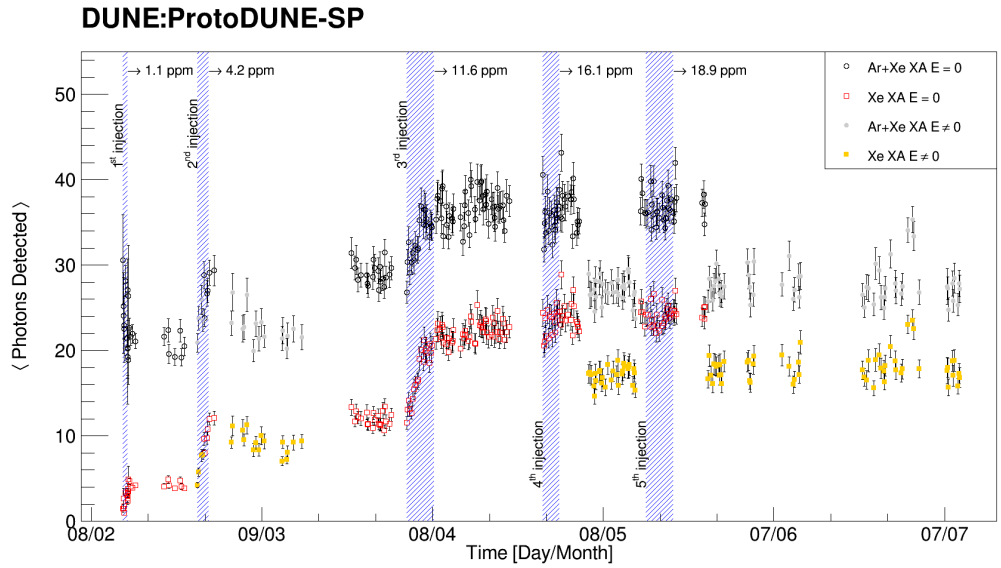

Figure 18: Light collected by the two X-ARAPUCA modules, in units of detected photons. The amount of collected light increases at each doping. Sudden drops are caused by the activation of the HV system of ProtoDUNE-SP and, hence, the presence of the electric field. Shaded areas show the time when Xe has been injected.

contamination could not be removed and thus persists throughout all xenon doping periods. The particulars of the contamination and injection are detailed in Section 2. All periods have, at different

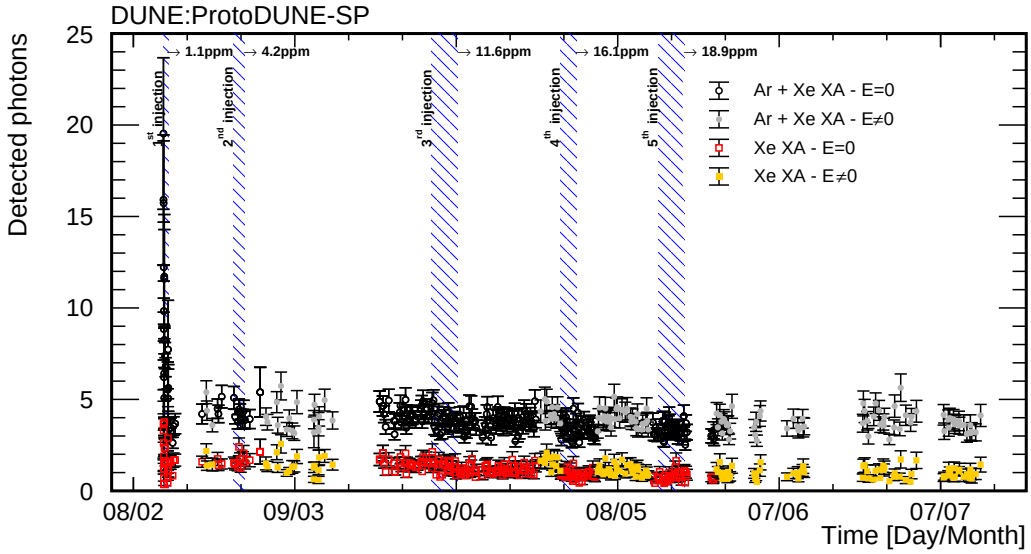

Figure 19: Time survey of the mean number of photons in the fast light component detected by the *Ar+Xe-XA* and by the *Xe-XA*, for runs with (E≠0) and without (E=0) electric field. The fast component is defined by setting a fixed time window, starting at the trigger time and encompassing the following 10 ticks. Shaded areas indicate Xe injections. Only events with at least three detected photons in the Ar+Xe X-ARAPUCA module are selected.

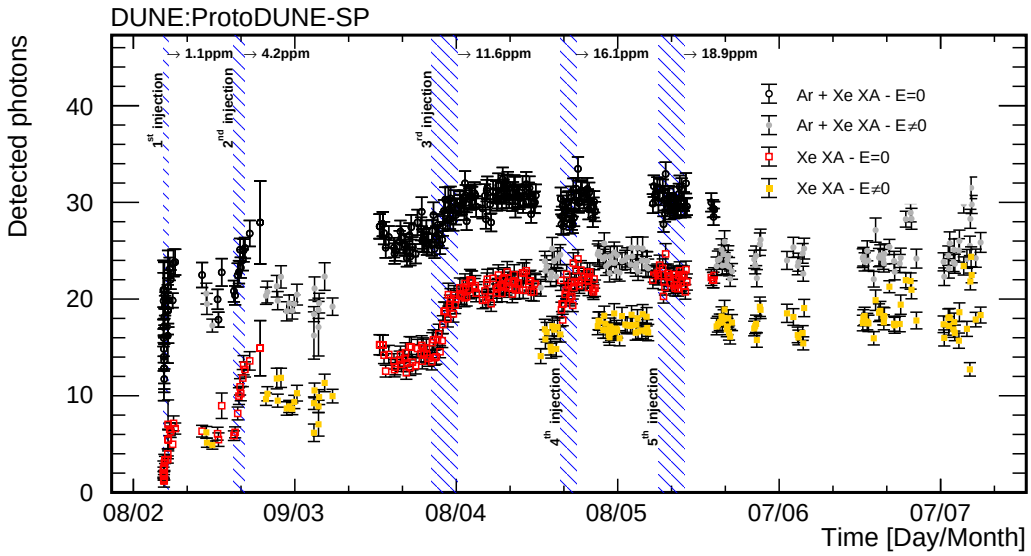

Figure 20: Time survey of the mean number of photons in the slow light component detected by the *Ar+Xe-XA* and by the *Xe-XA*, for runs with (E≠0) and without (E=0) electric field. The slow component is defined by setting a fixed time window, starting 11 ticks after the trigger time and encompassing the rest of the waveform. Shaded areas indicate Xe injections. Only events with at least three detected photons in the Ar+Xe X-ARAPUCA module are selected.

times, a number of values for the electric potential applied across the entire volume, ranging from no voltage to 180 kV (nominal electric field: 500 V/cm), and this significantly changes the amount of scintillation light available, as well as the triggering scheme appropriate for the collection of light. All of the following ProtoDUNE PDS studies use light collected from through-going cosmic-ray muons.

5.1 Triggering, data selection, and collected light

Triggering in ProtoDUNE-SP relies on the central DAQ and typically involves a coordination between two or more subsystems. For the ProtoDUNE-SP PDS, two major triggering schemes exist, which both depend on a coincidence between the upstream and downstream modules of the Cosmic-Ray Tagger (CRT). However, the trigger coincidence window length, pre-scaling, and trigger mask have varied throughout the run configurations as indicated by the red lines in each of the plots in Figure **??**. If the TPC is available and at the proper potential, a CRT coincidence is coordinated with through-going tracks, allowing a comparison of the orientation of the track, reconstructed by the TPC, to the vector which intersects the center of both triggered CRT modules strips. A quality cut is made on single tracks that meet the TPC reconstruction and selection criteria, have a viable trigger, and pass a quality cut of $\cos\theta > .999$, indicating a deviation of less than a degree between track from TPC and trigger from CRT. If the TPC is not available, a selection is made based on matching distinct PDS coincidences across APAs. At least two photon detectors in two different APAs must detect photons, within a time coincidence of 13 μs, in order for the event to be accepted within the analyzed light sample.

The light collected from the selected sample is summed across a single detector and assigned a radial distance, which is defined as the straight line distance from the exact center of the photon detector to the point along the track segment where the the center of the photon detector and the track are the same in the z-coordinate. A Gaussian or Poissonian fit to the collected light at each cm of radial distance is performed to obtain the most probable value, which represents the expected amount of light observed from a passing muon at a given radial distance. An analysis of the average collected light as a function of time and with different trigger periods is shown in Fig. **??**.

5.2 Light recovery due to Xenon injection

Attenuation curves, collected light ratios, and changes in the characteristic waveforms supply critical information about how the injected Xenon significantly alters the character of the scintillated light, as measured by the non-beam side ARAPUCA (Left TPC, or *Beam-Left*, BL, see Sec. 1, with respect to the beam direction.) in ProtoDUNE-SP. Fig. 25 clearly indicates that the amount of light measured by the non-beam side ARAPUCA increases significantly as compared to the N_2 contaminated period, and that the increase, as measured without electric field applied across the drift volume, tends to become larger at larger distances. This behavior is shown to persist in, as the electric field is applied across the drift volume for the operation of the TPC; however, the total magnitude of collected light is reduced, as a consequence of the recombination in the scintillation medium hindered by a non-zero electric field. This overall increase in light, with respect to the nitrogen contaminated period, is shown to persist across the entire ProtoDUNE-SP PDS, as demonstrated by the response of the double shifted light guides, shown in Fig. 26.

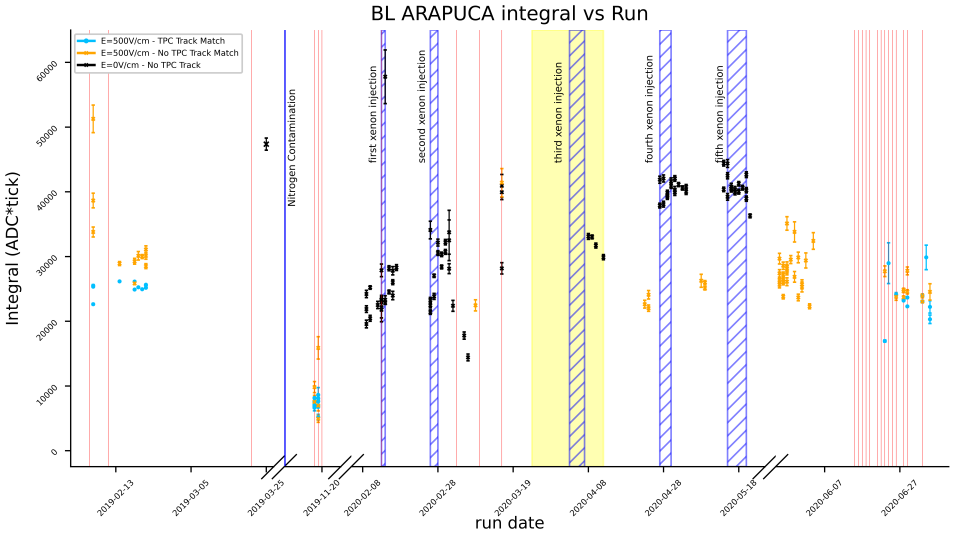

Figure 21: The figure shows the average amount of light collected from the ARAPUCA on beam left in the PDS over the entire nitrogen contamination and xenon doping period. In this plot, the red lines indicate changes in the trigger configurations, the blue lines indicate changes in the scintillation medium through nitrogen contamination or xenon injection, and the yellow period indicates a period of operation where only APA 3 and APA 6 were operational.

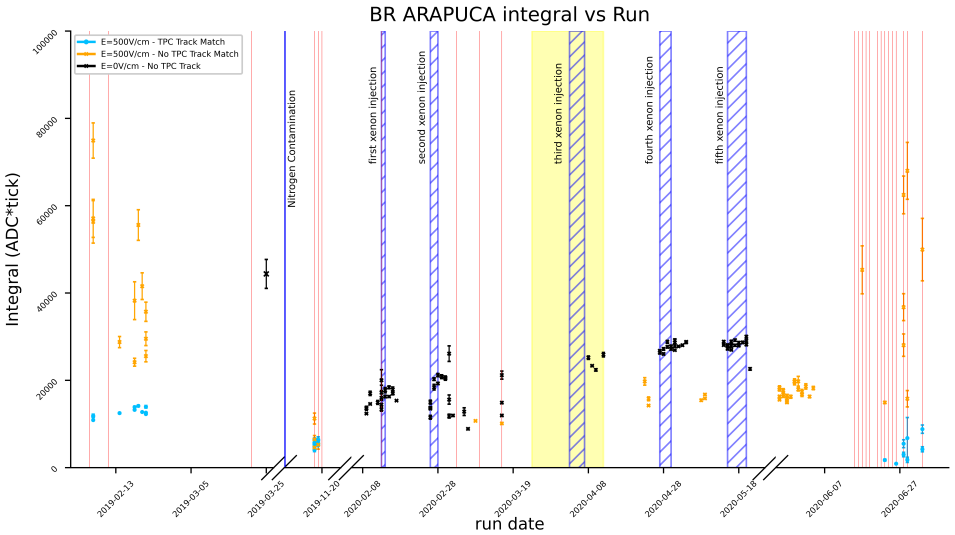

Figure 22: The figure shows the average amount of light collected from the ARAPUCA on beam right in the PDS over the entire nitrogen contamination and xenon doping period. In this plot, the red lines indicate changes in the trigger configurations, the blue lines indicate changes in the scintillation medium through nitrogen contamination or xenon injection, and the yellow period indicates a period of operation where only APA 3 and APA 6 were operational.

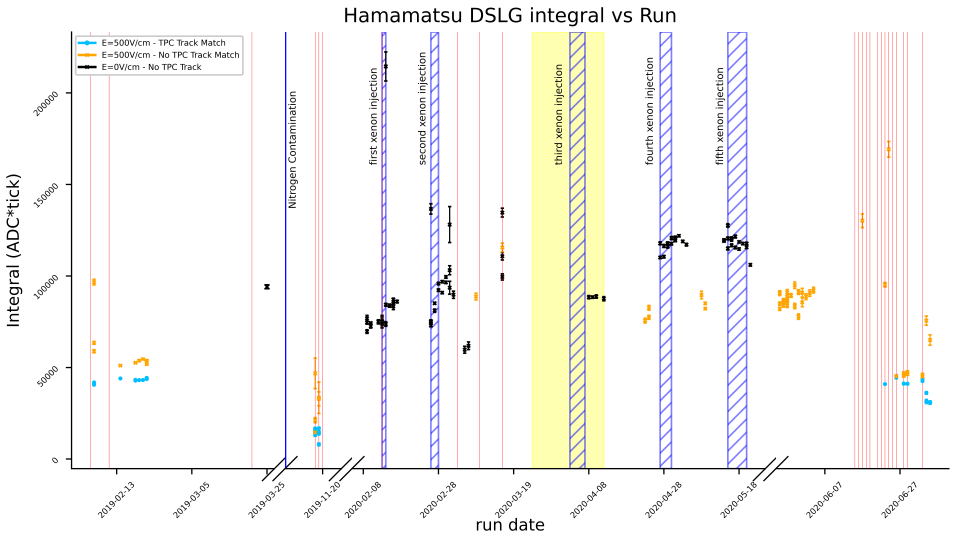

Figure 23: The figure shows the average amount of light collected from the Double shifted light guides with Hamamatsu MPPC sensors throughout the entire PDS over the entire nitrogen contamination and xenon doping period. In this plot, the red lines indicate changes in the trigger configurations, the blue lines indicate changes in the scintillation medium through nitrogen contamination or xenon injection, and the yellow period indicates a period of operation where only APA 3 and APA 6 were operational.

The details of the overall light increase with respect to the nitrogen contamination period is explained in the analysis of the characteristic waveform. Figure 27 demonstrates that, as the concentration of the Xenon dopant increases, the slow component of the characteristic Argon attenuation curve is increased by at least a factor of five, whereas a serious reduction of the characteristic Argon fast component appears as soon as the first doping. While the amount of light recovered across the detector is greater than what was seen with Nitrogen contamination, the introduction of the Xenon dopant recovers only about 95% of the light seen before the contamination.

Figures 25 (b,f) and 26 (bottom plots) confirm that, due to the larger Rayleigh length of Xenon w.r.t. the Argon light, the profile of the collected light versus the distance of the interaction from the detection plane increase the uniformity of response after the doping. This also mitigates the intrinsic non-uniformity of the DUNE PDS, which is installed only in the proximity of the TPC anode, i.e. inside the APAs.

6 Charge reconstruction in liquid Argon doped with Xe

A useful monitor of the stability of the ProtoDUNE TPC performance is the so-called *TPC signal strength*, i.e., the average amount of charge collected on the TPC collection wires during a standard run with cosmic rays. In ProtoDUNE-SP, the primary contribution to charge deposits in the LAr is ionization from cosmic rays. The amount of collected charge is evaluated for each collection wire by summing all the calibrated charge deposits, over those regions where the signal is significantly above the noise level for the channel. The fraction of the originally produced ionization charge

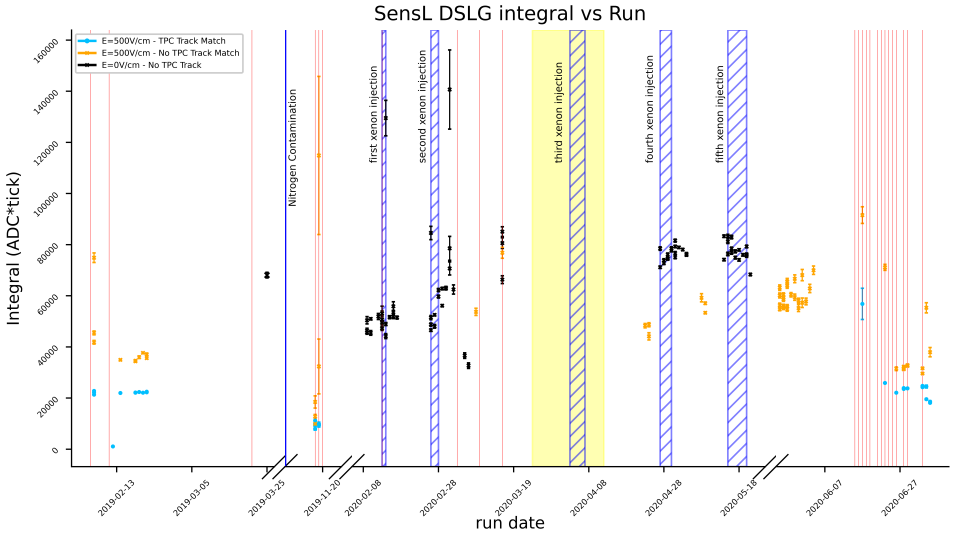

Figure 24: The figure shows the average amount of light collected from the Double shifted light guides with SensL SiPM sensors throughout the entire PDS over the entire nitrogen contamination and xenon doping period. In this plot, the red lines indicate changes in the trigger configurations, the blue lines indicate changes in the scintillation medium through nitrogen contamination or xenon injection, and the yellow period indicates a period of operation where only APA 3 and APA 6 were operational.

actually reaching each collection wire depends on the purity of the LAr, on the voltages applied to the wires, cathode planes and other TPC elements, as well as on space charge that accumulates in the LAr and on isolated detector elements. The calibrated response of the detector relies on the electronics modules gain, which was evaluated with test-charge injections and was stable over the course of the run [13].

Figure 28 shows the TPC signal strength before, during and after the Xenon filling, for those periods where APA data were collected with voltages at or near nominal values. Each point is evaluated by averaging the calibrated charge over all good collection wires in an APA for few thousand randomly triggered events, with acquisition windows of 3 ms in each event. The figure includes a line at 93 ke/channel/ms, typical for nominal voltages and high purity. Drops in signal strength on all APAs are due to episodes where the purity dropped. The response for APA-3 is always lower for the first few days after high voltage is turned on, because the grid plane that provides the shaping voltage for that APA was inadvertently disconnected and some time is required for it to passively charge up and be restored to proper functionality.

The Xenon doping period is highlighted in light yellow, whereas the darker yellow refers to maximal Xe concentration. The average TPC signal strength in standard conditions remains at its nominal value before, during and after the Xenon doping, indicating that the Xenon has no observable effect on the fraction of charge reaching the collection wires.

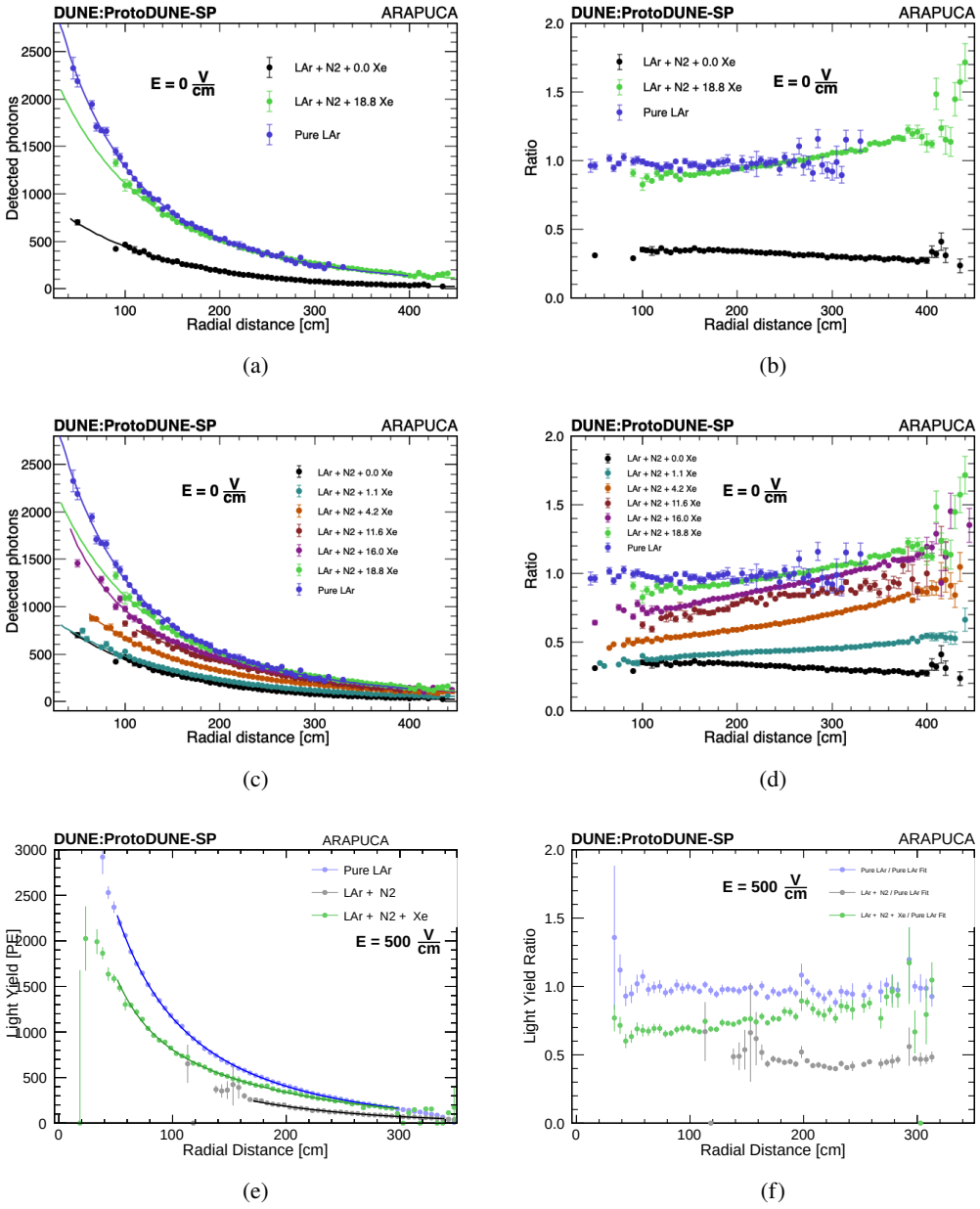

Figure 25: Light recovery demonstrated through attenuation curves after Xenon injection with the non-beam side PDS ARAPUCA. The left column of plots shows the light yield versus radial distance and the right column shows the ratio of collected light collected to the pure LAr and Nitrogen contaminated periods. The top row of plots show the measurement made with no potential across the volume, the middle plots show the gradual increase of light as increasing concentration of Xenon is achieved also with no potential volume, and the bottom row of plots shows the persistence of the light increase within the presence of the high potential necessary to operate the TPC.

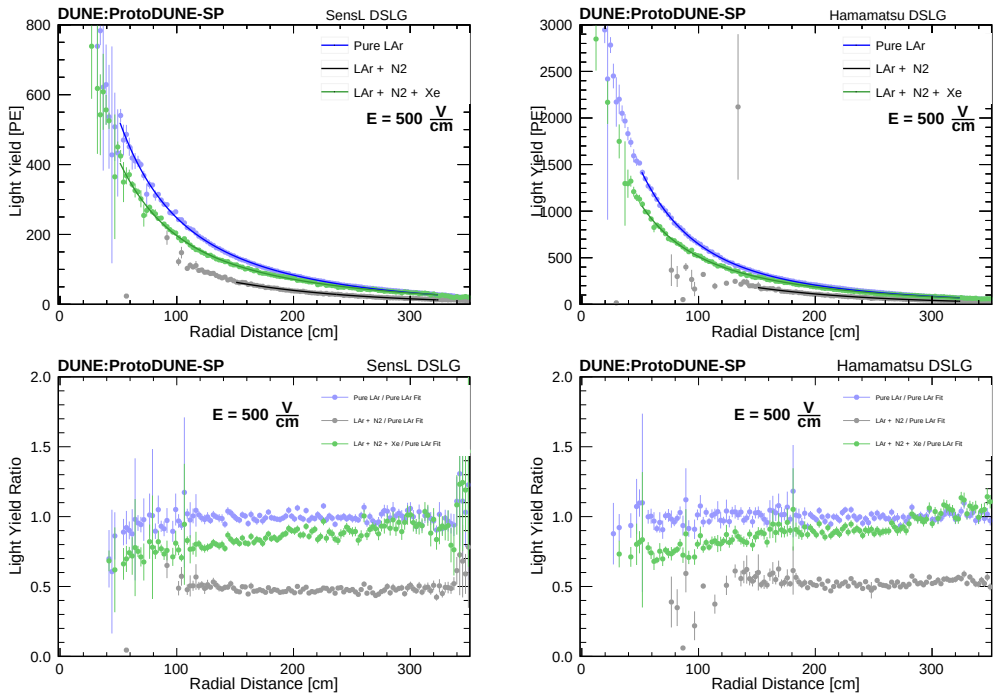

Figure 26: Light recovery as demonstrated through attenuation curves for the non-beam side double shifted light guides, divided by sensor technology. The top plots represent the light yield versus the radial distance and the bottom plots represent the light yield versus radial distance, normalized to the pure liquid argon case.

7 Conclusions

In this paper we presented the design, commissioning and analysis of the Xe-doping run of ProtoDUNE-SP. This run was performed in 2020 and represents the first demonstration that a large size (770 tons) LArTPC can be safely operated with Xenon at the level of $\sim$ 20 ppm. The performance of the detector were validated using both the built-in PDS and a dedicated X-ARAPUCA telescope triggered in standalone mode and installed before the run. Both systems provide consistent results: the 128 $\rightarrow$ 178 nm light shift is enabled already by Xe-concentrations of a few ppm and reach a plateau at $\sim$16 ppm. About 95% of the light originally lost due to Nitrogen pollution because of a failure in the recirculation system was recovered using this technique.

The data show that already at 10 ppm concentration most of the light that was lost due to the N_2 pollution of LAr is recovered, thanks to the shift of the excited states from Ar_2^* to Xe_2^*. In particular, the Ar_2^* triplet state is mostly affected by the pollution and the doping, being relatively long-lived. More detailed insights confirm that, due to the longer Rayleigh length of the Xenon light, the profile of the collected light versus the distance of the interaction from the detection plane is more uniform after the doping. These results are consistent between the runs with no electric field and the runs with electric field.

The analysis of the ionization charge collected by the anode planes during and after the Xe-doping demonstrates that Xenon up to 18.8 ppm does not affect the performance of the TPC.

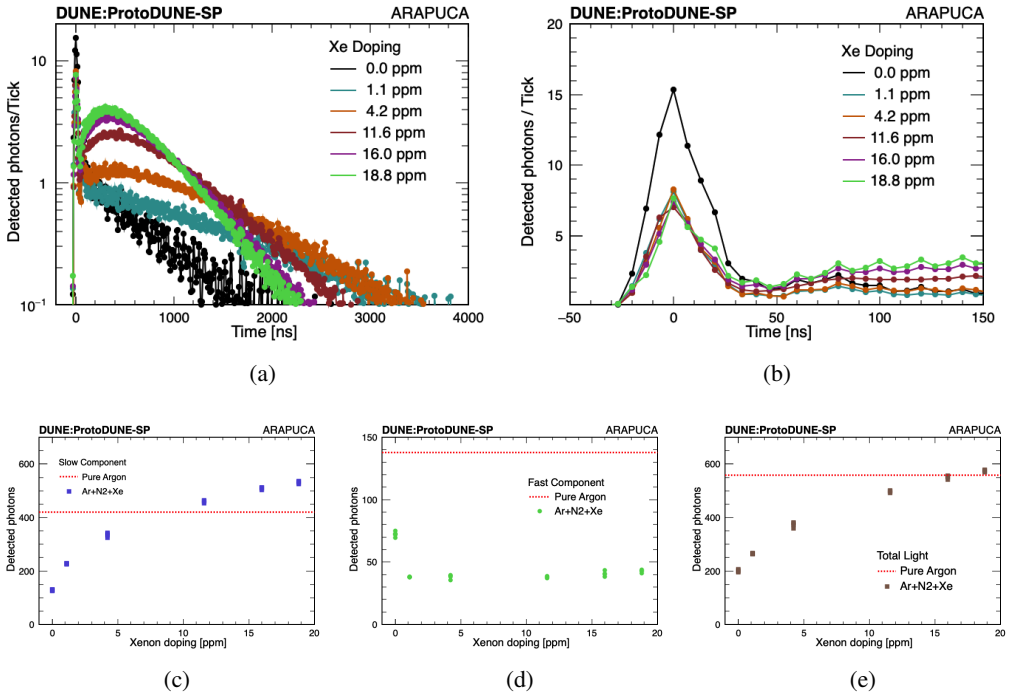

Figure 27: Non-Beam Side ARAPUCA deconvoluted waveforms at various concentrations of Xenon. The top plots show the characteristic waveform and how it changes at different concentrations of Xenon. The bottom plots show how the fast and slow component change as a function of Xenon concentration in the Nitrogen contaminated scintillation medium.
Events used in these plots are a subgroup of all events showed in Fig. 25 (c) and (d). Selection was made using tracks with a defined geometry. The selected events mean radial distance is ~ 250 cm and standard deviation ~ 30 cm. Given the differences between Ar and Xe light propagation, waveforms shape and integrals are expected to change with the event-detector distance, Figure 25.

The operation of doping with Xenon a LArTPC at the ~kt scale was a never attempted feat, and resulted in a smooth and successful run. The data collected during this campaign corroborates the use of Xenon to mitigate contamination risks during the DUNE data taking and the intrinsic non-uniformity of the PDS, which is installed only in the APA. These results will be extremely valuable to understand this operation mode for the DUNE far detector modules and other massive LArTPC.

References

[1] S. Amerio et al., "Design, construction and tests of the ICARUS T600 detector", *Nuclear Instruments and Methods in Physics Research Section A: Accelerators, Spectrometers, Detectors and Associated Equipment* **527** (2004), no. 3, 329–410, doi:https://doi.org/10.1016/j.nima.2004.02.044.

[2] R. Acciarri et al., "Design and construction of the MicroBooNE detector", *Journal of Instrumentation* **12** (feb, 2017) P02017–P02017, doi:10.1088/1748-0221/12/02/p02017.

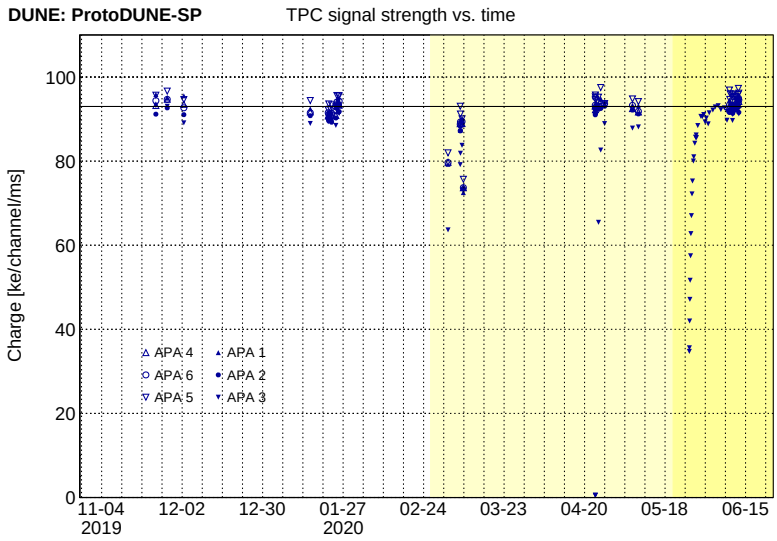

Figure 28: Signal strength vs. time near the time when Xenon was injected. The Xe doping period is highlighted in light yellow, whereas darker yellow represents Xenon at maximum concentration.

[3] C. Anderson et al., "The ArgoNeuT detector in the NuMI low-energy beam line at fermilab", *Journal of Instrumentation* **7** (oct, 2012) P10019–P10019, doi:10.1088/1748-0221/7/10/p10019.

[4] C. E. Aalseth et al., "Darkside-20k: A 20 tonne two-phase LAr TPC for direct dark matter detection at LNGS", *The European Physical Journal Plus* **133** (2018), no. 3, 131, doi:10.1140/epjp/i2018-11973-4.

[5] B. Abi et al., "Volume I. introduction to DUNE", *Journal of Instrumentation* **15** (aug, 2020) T08008–T08008, doi:10.1088/1748-0221/15/08/t08008.

[6] B. Abi et al., "Volume IV. the DUNE far detector single-phase technology", *Journal of Instrumentation* **15** (aug, 2020) T08010–T08010, doi:10.1088/1748-0221/15/08/t08010.

[7] S. Kubota, M. Hishida, M. Suzuki, and J. Ruan(Gen), "Liquid and solid argon, krypton and xenon scintillators", *Nuclear Instruments and Methods in Physics Research* **196** (1982) 101–105.

[8] M. Suzuki, M. Hishida, J. Ruan(Gen), and S. Kubota, "Light output and collected charge in xenon-doped liquid argon.", *Nuclear Instruments and Methods in Physics Research* **A327** (1993) 67–70.

[9] M. Hofmann et al., "Ion-beam excitation of liquid argon.", *The European Physics Journal* **C73** (oct, 2013) 2618, doi:10.1140/epjc/s10052-013-2618-0.

[10] C. Wahl et al., "Pulse-shape discrimination and energy resolution of a liquid-argon scintillator with xenon doping.", *Journal of Instrumentation* **9** (2014) P06013, doi:10.1088/1748-0221/9/06/P06013.

[11] D. Akimov et al., "Fast component re-emission in xe-doped liquid argon.", *Journal of Instrumentation* **14** (sep, 2019) P09022, doi:10.1088/1748-0221/14/09/P09022.

[12] B. Abi et al., "First results on ProtoDUNE-SP liquid argon time projection chamber performance from a beam test at the CERN neutrino platform", *Journal of Instrumentation* **15** (dec, 2020) P12004–P12004, doi:10.1088/1748-0221/15/12/p12004.

[13] D. Adams et al., "The ProtoDUNE-SP LArTPC electronics production, commissioning, and performance", *Journal of Instrumentation* **15** (jun, 2020) P06017–P06017, doi:10.1088/1748-0221/15/06/p06017.

[14] B. Howard et al., "A Novel Use of Light Guides and Wavelength Shifting Plates for the Detection of Scintillation Photons in Large Liquid Argon Detectors", *Nucl. Instrum. Meth.* **907** (2018) 9–21, doi:10.1016/j.nima.2018.06.050, arXiv:1710.11233.

[15] L. Bugel et al., "Demonstration of a Lightguide Detector for Liquid Argon TPCs", arXiv:1101.3013.

[16] Z. Moss et al., "A Factor of Four Increase in Attenuation Length of Dipped Lightguides for Liquid Argon TPCs Through Improved Coating", arXiv:1604.03103.

[17] A. Machado and E. Segreto, "ARAPUCA a new device for liquid argon scintillation light detection", *Journal of Instrumentation* **11** (feb, 2016) C02004–C02004, doi:10.1088/1748-0221/11/02/c02004.

[18] A. Machado et al., "The X-ARAPUCA: an improvement of the ARAPUCA device", *Journal of Instrumentation* **13** (apr, 2018) C04026–C04026, doi:10.1088/1748-0221/13/04/c04026.

[19] C. Brizzolari et al., "Enhancement of the X-Arapuca photon detection device for the DUNE experiment", arXiv:2104.07548.

[20] R. Acciarri et al., "Effects of nitrogen contamination in liquid argon", *Journal of Instrumentation* **5** (jun, 2010) P06003–P06003, doi:10.1088/1748-0221/5/06/p06003.

[21] T. Heindl et al., "Table-top setup for investigating the scintillation properties of liquid argon", *Journal of Instrumentation* **6** (feb, 2011) P02011–P02011, doi:10.1088/1748-0221/6/02/p02011.

[22] Aprile, E. et al., "The xenon1t dark matter experiment", *Eur. Phys. J. C* **77** (2017), no. 12, 881, doi:10.1140/epjc/s10052-017-5326-3.

[23] D. Akerib et al., "The large underground xenon (lux) experiment", *Nuclear Instruments and Methods in Physics Research Section A: Accelerators, Spectrometers, Detectors and Associated Equipment* **704** (2013) 111–126, doi:https://doi.org/10.1016/j.nima.2012.11.135.

[24] A. Buzulutskov, "Photon emission and atomic collision processes in two-phase argon doped with xenon and nitrogen.", *Europhysics Letters* **17** (mar, 2017) 39002, doi:10.1209/0295-5075/117/39002.

[25] E. Voirin, "ProtoDUNE LAr Flow Simulation- Impurity field and Charge Density.", Technical Report DUNE DocDB Doc # 928, Jun, 2019.

[26] M. Corbetta, R. Guida, and B. Mandelli, "Gas chromatograph and mass spectrometer analysis of Xenon bottles used by the ProtoDUNE Experiment.", Technical Report CERN EP-DT-FS, Mar, 2020.

[27] G. Bakale, U. Sowada, and W. F. Schmidt, "Effect of an electric field on electron attachment to sulfur hexafluoride, nitrous oxide, and molecular oxygen in liquid argon and xenon.", *The Journal of Physical Chemistry* **80** (nov, 1976) 2556–2559, doi:10.1021/j100564a006.

[28] E. Segreto et al., "First liquid argon test of the X-ARAPUCA", *Journal of Instrumentation* **15** (may, 2020) C05045–C05045, doi:10.1088/1748-0221/15/05/c05045.

[29] "OPTO webpage". http://opto.com.br/.

[30] Eljen Technology, "Wavelength Sifting Plastics EJ-280, EJ-282, EJ-284, EJ-286", https://eljentechnology.com/products/wavelength-shifting-plastics/ej-280-ej-282-ej-284-ej-286.

[31] Hamamatsu, "MPCC S13360-2050VE/3050VE/6050VE", https://www.hamamatsu.com/eu/en/product/type/S13360-6050VE/index.html.

[32] DUNE Collaboration, "The Single-Phase ProtoDUNE Technical Design Report. ", Technical Report FERMILAB-DESIGN-2017-02, Jun, 2017. 165 pages.

[33] M. Morháč et al., "Background elimination methods for multidimensional coincidence γ-ray spectra", *Nuclear Instruments and Methods in Physics Research Section A: Accelerators, Spectrometers, Detectors and Associated Equipment* **401** (1997), no. 1, 113–132, doi:https://doi.org/10.1016/S0168-9002(97)01023-1.